

The heavy neutral Higgs signature in the $\gamma\gamma \rightarrow ZZ$ process.[†]

G.J. Gounaris^a, P.I. Porfyriadis^a and F.M. Renard^b

^aDepartment of Theoretical Physics, Aristotle University of Thessaloniki,
Gr-54006, Thessaloniki, Greece.

^bPhysique Mathématique et Théorique, UMR 5825
Université Montpellier II, F-34095 Montpellier Cedex 5.

Abstract

If the Standard Model (SM) Higgs particle is sufficiently heavy, then its contribution to $\gamma\gamma \rightarrow ZZ$ should be largely imaginary, interfering with the predominantly imaginary W -loop generated SM "background". We find that for standard model Higgs masses in the region $200 \lesssim m_H \lesssim 500$ GeV, this interference is indeed constructive and increases the Higgs signal. In the minimal SUSY case an interference effect should also appear for the contribution of the heavier CP-even neutral Higgs boson H^0 , provided it is sufficiently heavy. This effect is somewhat reduced though, by the smallness of the H^0 width and the $\gamma\gamma$ and ZZ branching ratios. In any case, this interference is found constructive for part of the parameter space corresponding to sfermion masses at the TeV scale and maximal stop mixing. For both the SM and SUSY cases, regions of the parameter space exist though, where the interference may be destructive. It is therefore essential to take these effects into account when searching for possible scalar Higgs-like candidates. For that purpose we present the complete analytic expressions for both resonance and background amplitudes.

[†]Partially supported by the European Community grant HPRN-CT-2000-00149.

1 Introduction

Searching for the Higgs particle(s) is definitely the central aim in particle physics at present. If the Standard Model (SM) correctly describes nature, then the present LEP results require the Higgs mass to be heavier than 113 GeV [1]. This constraint is somewhat loosened in minimal SUSY, in which for typical scenarios assuming sfermion masses at the TeV scale and maximal stop mixing, the lower bound on the mass of the lightest CP-even neutral Higgs h^0 is reduced to about 90 GeV, and the $\tan\beta$ -region ($0.5 - 2.3$) is excluded [1].

After the discovery of the Higgs particle(s), the necessity will of course arise to secure its identification. To this aim, a photon-photon Collider ($LC_{\gamma\gamma}$) realized through the laser backscattering method [3] in a high luminosity e^-e^- or e^+e^- Collider (LC) [4], should be very useful. In an $LC_{\gamma\gamma}$ the neutral Higgs particle may then be produced directly in the s -channel, and if it is not too narrow, even its line shape may be studied.

For a standard model (SM) light Higgs boson (i.e. $m_H \lesssim 135$ GeV) the rate of direct production in $\gamma\gamma \rightarrow H$ is indeed very high and the detection of the Higgs boson should clearly be done through the dominant decay channel $H \rightarrow b\bar{b}$ [2, 5]. For higher Higgs masses though, the situation changes because the Higgs becomes broader and the dominant channels are now WW and ZZ . A very interesting channel for Higgs detection is then the ZZ one, in which at least one Z decays into lepton pairs and the other one into hadrons or leptons. Such a channel will be very useful, even though $Br(H \rightarrow \gamma\gamma)$ decreases rapidly as the Higgs mass increases.

However, to this $\gamma\gamma \rightarrow H \rightarrow ZZ$ channel, there is an important $\gamma\gamma \rightarrow ZZ$ background process arising mainly through W and fermions box-type contributions [6, 7, 8]. As emphasized in [8], this background process has the remarkable property that at high energies its predominant helicity amplitudes are almost purely imaginary and conserve helicity¹. So clear interference effects between the Higgs and background contributions are expected, which should be taken into account when analyzing experimental data.

The first aim of this paper is to explore this interference phenomenon in SM for Higgs masses above the ZZ production threshold, using the already known one-loop $\gamma\gamma \rightarrow ZZ$ amplitudes [6, 7, 8].

We next turn to a general MSSM model [11], assuming no CP violation other than the standard one included in the Yukawa sector. In this case, the Higgs boson spectrum is much richer, with two CP-even scalars h^0 , H^0 and one CP-odd pseudoscalar A^0 [12]. We consider SUSY scenarios in which H^0 and A^0 are heavier than about 200 GeV, while the SUSY breaking sfermion parameters are taken at the TeV scale and the stop mixing is maximal. Such scenarios have the tendency to lead to an h^0 which is well within the presently experimentally allowed region [1]. The lightest Higgs boson vertex $h^0\gamma\gamma$ for SUSY models, has recently been studied in [13]. Since the CP-odd A^0 has no tree-level coupling to $\gamma\gamma$ or ZZ , the $\gamma\gamma \rightarrow ZZ$ channel may be used (as in the SM case above) for the on-shell production of the CP-even Higgs H^0 .

¹A similar property has also been observed for the processes $\gamma\gamma \rightarrow \gamma\gamma$, γZ at sufficiently high energies [9, 10].

Apart from the existence of the lighter Higgs h^0 , there are several new features discriminating the heavier SUSY H^0 boson, from the case of a heavy standard Higgs. The decay spectrum of the SUSY H^0 is expected to differ from that of a heavy standard Higgs, because of the possible appearance of new decay channels and mixing effects which strongly influence its couplings to gauge bosons. Thus for $m_{H^0} \gtrsim 200\text{GeV}$, the SUSY H^0 is expected to be much narrower than a heavy standard H , and its branching ratios $Br(H^0 \rightarrow \gamma\gamma)$ and $Br(H^0 \rightarrow ZZ)$ much smaller [12, 14]. Moreover, in an MSSM description, the $\gamma\gamma \rightarrow ZZ$ background receives at one loop new contributions from virtual SUSY partners running inside the loop [8]. So finally, within the MSSM, the treatment of the Higgs effects in the $\gamma\gamma \rightarrow ZZ$ process requires a specific analysis. This constitutes the second topic of this paper.

In Section 2 we write the Higgs contributions to the $\gamma\gamma \rightarrow ZZ$ amplitudes for the SM (H) and for the MSSM (h^0 , H^0) cases. We give the explicit expressions of the one loop Higgs couplings to $\gamma\gamma$ and the tree level couplings to ZZ . In the Appendix we collect all background amplitudes for $\gamma\gamma \rightarrow ZZ$ arising in SM and in MSSM. They are taken from [8], except for the mixed chargino box contributions arising when two different charginos are running along the box loop, which had not been computed before. In Section 3 we compute the polarized $\gamma\gamma \rightarrow ZZ$ differential cross section induced by the above Higgs and background contributions. We discuss the shape of the ZZ invariant mass distribution and the observability of the Higgs signal, taking into account the energy spread of the $\gamma\gamma$ initial state. We give various illustrations with heavy SM and MSSM Higgs particles. The results are summarized and commented in the concluding Section 4.

2 The Higgs contribution to the $\gamma\gamma \rightarrow ZZ$ amplitudes.

As in [8, 9, 10], we use the non-linear Feynman gauge in which there are two sets of diagrams contributing to $\gamma\gamma \rightarrow ZZ$ [15]; compare Fig.1. The first consists of the one-particle irreducible "box"-diagrams involving two photons and two Z 's as external legs; see Fig.1a. Their contributions, arising from loops involving W 's [7], quarks and leptons and charginos [6], as well as charged Higgs particles and sfermions [8], are summarized in the Appendix. We note in particular that the "mixed" chargino boxes, induced by the $Z\tilde{\chi}_1\tilde{\chi}_2$ couplings involving two different charginos, are presented in (A.36, A.51-A.66). Numerically, they are not expected to be particularly important. Nevertheless, we list them here for completeness, because their derivation (including their simplification to the present form) required a considerable effort. The analogous "mixed" sfermion box contributions have not been calculated, since they should be at most of similar magnitude to the single sfermion, which is already known to be very small [8].

The second set of diagrams² depicted in Fig.1b, consists of those involving contributions from a Higgs pole in the s -channel. These diagrams contain a Higgs- $\gamma\gamma$ vertex

²Notice that as opposed to the previous set, these are one-particle reducible diagrams.

generated by loops along which W -gauge bosons and fermion or scalar particles are running. Their general form is

$$F_{\lambda_1\lambda_2\lambda_3\lambda_4}^h(\gamma\gamma \rightarrow ZZ) = -\frac{\alpha^2}{2s_W^2 c_W^2} \left\{ \mathcal{H}(s) \right\} \cdot \frac{(1+\lambda_1\lambda_2)}{2} \left[(1+\lambda_3\lambda_4) \frac{\lambda_3\lambda_4}{2} - \frac{1+\beta_Z^2}{1-\beta_Z^2} (1-\lambda_3^2)(1-\lambda_4^2) \right] . \quad (1)$$

In SM, where only one physical neutral Higgs particle exists with mass m_H , we have

$$\mathcal{H}(s) = \sum_i N_i^c Q_i^2 \mathcal{F}_i(\tau) \frac{s}{s - m_H^2 + im_H \Gamma_H} , \quad (2)$$

where the index i runs over the physical charged particles with spin (1, 1/2) running along the loop with their interactions determined by [12]

$$\mathcal{L}_{H^0(SM)} = gm_W W_\mu^+ W^{\mu-} H^0 - \frac{gm_f}{2m_W} \bar{\psi}_f \psi_f H^0 - \frac{gm_H^2}{2m_W} G^+ G^- H^0 , \quad (3)$$

and their respective contributions to $H^0\gamma\gamma$ by

$$\mathcal{F}_1(\tau) = \frac{2m_H^2}{s} + 3\tau + 3\tau \left(\frac{8}{3} - \frac{2m_H^2}{3s} - \tau \right) f(\tau) , \quad (4)$$

$$\mathcal{F}_{1/2}(\tau) = -2\tau[1 + (1-\tau)f(\tau)] , \quad (5)$$

where

$$\tau = \frac{4m_i^2}{s} , \quad f(\tau) = -\frac{s}{2} C_0(0, 0, s; m_i, m_i, m_i) , \quad (6)$$

with³ C_0 being the standard Passarino-Veltman function [16] in the notation of [8, 17]; (compare (A.37-A.46)). In (2), Q_i is the charge and N_i^c the colour multiplicity of the particle contributing to $H^0\gamma\gamma$ loop.

The most important contributions to (2) in SM come from W^\pm (to which Goldstone and FP ghost are always included) and the top-loop, which are determined by (4) and (5) respectively.

It is also useful to remark that if a physical scalar charged particle H^\pm with mass m_{H^\pm} were introduced in SM interacting with the physical neutral Higgs as [12]

$$\mathcal{L}_{H^0 H^+ H^-} = -\frac{gm_{H^\pm}^2}{m_W} H^+ H^- H^0 , \quad (7)$$

then an additional contribution would arise in (2) determined by the function

$$\mathcal{F}_0(\tau) = \tau[1 - \tau f(\tau)] , \quad (8)$$

³A simple expression for C_0 in terms of logarithms may be seen *e.g.* in Eqs.(B.2) of [8].

which is analogous to those in (4, 5) and determines the contributions to $H\gamma\gamma$ from spin=0 charged particles running along the loop [12]. It may then be instructive to notice that the standard W^\pm contribution (4) can be written as

$$\mathcal{F}_1(\tau) = 3\tau \left[1 + \left(\frac{8}{3} - \tau \right) f(\tau) \right] + \frac{m_H^2}{2m_W^2} \mathcal{F}_0(\tau) . \quad (9)$$

In the Feynmann gauge, the first term in (9) gives the pure W and ghost SM contributions, while the last term (having exactly the structure that would be induced by a scalar charged particle of mass m_W) describes the Goldstone one. But of course, such a separation is not gauge invariant.

In the MSSM case, with no additional CP-violating phases in the new physics sector, there will be two neutral CP-even Higgs particles (h^0 , H^0) contributing to (1) so that

$$\begin{aligned} \mathcal{H}(s) = & \sum_i N_i^c Q_i^2 \left[\sin(\beta - \alpha) \mathcal{F}_i^{h^0}(\tau) \frac{s}{s - m_{h^0}^2 + im_{h^0} \Gamma_{h^0}} \right. \\ & \left. + \cos(\beta - \alpha) \mathcal{F}_i^{H^0}(\tau) \frac{s}{s - m_{H^0}^2 + im_{H^0} \Gamma_{H^0}} \right] , \end{aligned} \quad (10)$$

where the sum is running over the physical charged particles with spin (1, 1/2, 0) contributing to the $h^0\gamma\gamma$ and $H^0\gamma\gamma$ vertices; these are W^\pm (to which G^\pm and FP ghosts are always included), as well as charginos $\tilde{\chi}^\pm$, H^\pm and sfermions \tilde{f}_j . The interaction Lagrangian determining the necessary couplings is

$$\begin{aligned} \mathcal{L}_{(h^0, H^0)(\text{SUSY})} = & gm_W [H^0 \cos(\beta - \alpha) + h^0 \sin(\beta - \alpha)] \left\{ W^{-\mu} W_\mu^+ + \frac{1}{2c_W^2} Z^\mu Z_\mu - H^+ H^- \right\} \\ & + \frac{gm_W}{2c_W^2} \cos 2\beta [h^0 \sin(\alpha + \beta) - H^0 \cos(\alpha + \beta)] (G^+ G^- - H^+ H^-) \\ & - \frac{gm_t}{2m_W \sin \beta} [H^0 \sin \alpha + h^0 \cos \alpha] \bar{t}t - \frac{g}{2m_W \cos \beta} [H^0 \cos \alpha - h^0 \sin \alpha] (m_b \bar{b}b + m_\tau \bar{\tau}\tau) \\ & - \frac{gm_t^2}{m_W \sin \beta} [h^0 \cos \alpha + H^0 \sin \alpha] (\tilde{t}_1^* \tilde{t}_1 + \tilde{t}_2^* \tilde{t}_2) - \frac{gm_t}{2m_W \sin \beta} [h^0 (A_t \cos \alpha + \mu \sin \alpha) \\ & + H^0 (A_t \sin \alpha - \mu \cos \alpha)] \sin(2\theta_t) \text{Sign}(A_t - \mu \cot \beta) (\tilde{t}_1^* \tilde{t}_1 - \tilde{t}_2^* \tilde{t}_2) \\ & - \frac{gm_W}{c_W^2} [H^0 \cos(\alpha + \beta) - h^0 \sin(\alpha + \beta)] \left\{ \left[\frac{2s_W^2}{3} + \left(\frac{1}{2} - \frac{4s_W^2}{3} \right) \cos^2 \theta_t \right] \tilde{t}_1^* \tilde{t}_1 \right. \\ & \left. + \left[\frac{2s_W^2}{3} + \left(\frac{1}{2} - \frac{4s_W^2}{3} \right) \sin^2 \theta_t \right] \tilde{t}_2^* \tilde{t}_2 \right\} \\ & - \frac{g}{\sqrt{2}} \tilde{\Delta}_1 \left[\tilde{\mathcal{B}}_L \cos \phi_R \sin \phi_L (H^0 \cos \alpha - h^0 \sin \alpha) + \tilde{\mathcal{B}}_R \sin \phi_R \cos \phi_L (H^0 \sin \alpha + h^0 \cos \alpha) \right] \tilde{\chi}_1 \tilde{\chi}_1 \\ & + \frac{g}{\sqrt{2}} \tilde{\Delta}_2 \left[\tilde{\mathcal{B}}_R \sin \phi_R \cos \phi_L (H^0 \cos \alpha - h^0 \sin \alpha) \right. \\ & \left. + \tilde{\mathcal{B}}_L \sin \phi_L \cos \phi_R (H^0 \sin \alpha + h^0 \cos \alpha) \right] \tilde{\chi}_2 \tilde{\chi}_2 . \end{aligned} \quad (11)$$

The implied W -loop contributions to the h^0 , H^0 terms in (10) (to which Goldstone and ghost are always included) are then respectively

$$\mathcal{F}_1^{h^0}(\tau) = \sin(\beta - \alpha) 3\tau \left[1 + \left(\frac{8}{3} - \tau \right) f(\tau) \right] - \frac{\cos(2\beta) \sin(\beta + \alpha)}{2c_W^2} \mathcal{F}_0(\tau), \quad (12)$$

$$\mathcal{F}_1^{H^0}(\tau) = \cos(\beta - \alpha) 3\tau \left[1 + \left(\frac{8}{3} - \tau \right) f(\tau) \right] + \frac{\cos(2\beta) \cos(\beta + \alpha)}{2c_W^2} \mathcal{F}_0(\tau), \quad (13)$$

while the contributions from fermion and physical scalar particles are given by (5, 8) respectively, after substituting of course the obvious changes in the couplings implied by (3, 7) and (11).

Concerning the parameters entering (11), we first quote the neutral Higgs mixing angle α determined by [11]

$$\tan(2\alpha) = \tan(2\beta) \frac{m_{A^0}^2 + m_Z^2}{m_{A^0}^2 - m_Z^2 + \frac{\epsilon}{\cos(2\beta)}}, \quad (14)$$

and the constraint $-\pi/2 \leq \alpha \leq 0$. The leading top-stop contribution to (14) is [18]

$$\epsilon \simeq \frac{3G_F m_t^4}{\sqrt{2}\pi^2 \sin^2 \beta} \ln \left(\frac{M_S^2}{m_t^2} \right), \quad (15)$$

where $M_S^2 \simeq m_{\tilde{t}_1} m_{\tilde{t}_2}$ provides a measure of the SUSY breaking scale.

We also note that the neutral Higgs- \tilde{t}_i couplings in (11) depend on the $(\tilde{t}_L, \tilde{t}_R)$ mixing defined in (A.19, A.18); while the neutral Higgs-chargino couplings in (11), assume the mixing definition in (A.26-A.30) and the sign quantities $\tilde{\Delta}_1$, $\tilde{\Delta}_2$, $\tilde{\mathcal{B}}_L$ and $\tilde{\mathcal{B}}_R$ given in (A.35). The consistency of the formalism guarantees that the chargino physical masses are always positive, for any sign of M_2 and μ .

3 The $\gamma\gamma \rightarrow ZZ$ signal around the Higgs pole.

Since we seek to study the contribution of a Higgs s -channel pole, it is advantageous to use polarized electron and laser beams with opposite helicities. This ensures a high monochromaticity and (circular) polarization for the photon beams. Thus, in the following we choose the helicities of both photons in $LC_{\gamma\gamma}$ to be $\lambda_1 = \lambda_2 = 1$, so that the accessible differential cross section is⁴

$$\frac{d\sigma_{++}(\gamma\gamma \rightarrow ZZ)}{d\cos\vartheta^*} = \left(\frac{\beta_Z}{64\pi s} \right) \sum_{\lambda_3\lambda_4} |F_{++\lambda_3\lambda_4}|^2, \quad (16)$$

to which the Higgs pole contributes most strongly.

⁴The statistics factor due to the two Z 's in the final state has been taken into account so that $-1 < \cos\vartheta^* < 1$.

If the width of the Higgs particle we are interested to study is smaller than the energy resolution, as it happens for either SM or SUSY Higgs particles in the range (200 – 300) GeV, and if the LC energy is tuned close to the maximum of the polarized photon flux; then the number of expected events is determined by an effective differential luminosity which may be bigger than [5, 3, 19]

$$\frac{d\mathcal{L}^{\gamma\gamma}}{dw} \simeq 1 \frac{\text{fb}^{-1}}{\text{GeV}} . \quad (17)$$

In (17), $w \equiv \sqrt{s_{\gamma\gamma}} \simeq m_H$, where m_H is the mass of the neutral Higgs particle we are interested to study; and $\mathcal{L}_{ee} \simeq 200 \text{ fb}^{-1}$ has been assumed [20].

Assuming that the energy resolution of an $LC_{\gamma\gamma}$ is around 10 GeV, then the number of $\gamma\gamma \rightarrow ZZ$ events expected in the mass region of a narrow Higgs particle is [3, 14, 5]

$$\mathcal{N} \simeq \left(\frac{d\mathcal{L}^{\gamma\gamma}}{dw} \right)_{w=m_H} \cdot I_f \cdot \int_{m_H-5\text{GeV}}^{m_H+5\text{GeV}} dw \sigma_{++}(\gamma\gamma \rightarrow ZZ) , \quad (18)$$

while the number of "background" events that would had been expected in the same energy region if the Higgs pole had been removed and we had smoothly joined the cross sections below and above the Higgs peak, would had been

$$\mathcal{N}_{Bg} \simeq \left(\frac{d\mathcal{L}^{\gamma\gamma}}{dw} \right)_{w=m_H} \cdot I_f \cdot \int_{m_H-5\text{GeV}}^{m_H+5\text{GeV}} dw \sigma_{++}(\gamma\gamma \rightarrow ZZ; \text{background}) . \quad (19)$$

This later number is introduced as a definition of the background, in order to describe quantitatively the significance of the Higgs signal. The quantity I_f in (18, 21) denotes the identification factor of the Z -pair. Assuming that the useful modes for the ZZ identification are those where one Z decays leptonically (including the invisible neutrino mode), and the other hadronically, we get $I_f \simeq 0.47$; while if only charged leptons are used for the leptonic mode, $I_f \simeq 0.14$ is obtained. In the following we optimistically use $I_f = 0.47$.

As a first application we turn to the SM case, taking⁵ $m_H = 300 \text{ GeV}$ and $\Gamma_H = 8.51 \text{ GeV}$ [23]. The implied $\sigma_{++}(\gamma\gamma \rightarrow ZZ)$ cross section integrated in the angular region $30^\circ < \vartheta^* < 150^\circ$ is presented in Fig.2a. For orientation, the SM cross section computed with $m_H = 100 \text{ GeV}$ is also given for values around $w \equiv \sqrt{s_{\gamma\gamma}} \simeq 300 \text{ GeV}$. Then, from (18) we find

$$\mathcal{N}^{SM} \simeq 5652 I_f \simeq 2656 \text{ events} , \quad (20)$$

while (19) gives

$$\mathcal{N}_{Bg}^{SM} \simeq 600 I_f \simeq 282 \text{ events} , \quad (21)$$

so that

$$S.D. \equiv \frac{(\mathcal{N}^{SM} - \mathcal{N}_{Bg}^{SM})}{\sqrt{\mathcal{N}_{Bg}^{SM}}} \simeq 141 , \quad (22)$$

⁵We note in passing that standard model Higgs masses of up to 500 GeV, or even larger, may easily be made consistent with all experimental data and theoretical bounds, by either introducing new very heavy particles or extra large dimension. For a review see [21].

provides a definition of the number of the standard deviations of the effect. Thus, in the SM case for moderately large Higgs masses, the effect is indeed very conspicuous. Note that S.D., the number of the standard deviations, depends on the Z identification factor through $\sqrt{I_f}$, so that if we had used $I_f = 0.14$, it would have been reduced only by a factor 2.

We should also remark here that the enhancement around the Higgs mass indicated in Fig.2a and (20, 21), is not only due to the magnitude of the Higgs contribution close to its mass shell, but also due to its constructive interference with the predominantly imaginary F_{++++} amplitude induced by the W -loop [8]. We find that such a constructive interference remains true around $w \simeq m_H$ for Higgs masses up to ~ 460 GeV. For higher m_H though, the interference starts becoming destructive.

This change of the interference pattern is clearly seen in Fig.2b where $m_H = 500$ GeV and $\Gamma_H = 67.53$ GeV are used [23]. As always, but particularly in this case, a suitable binning of the data would be very helpful in enhancing the effect and reducing the background. Thus, if we *e.g.* select as signal region the one between 400 and 512 GeV (instead of the one between $m_H - 5$ GeV and $m_H + 5$ GeV), then the number of events becomes $\mathcal{N}^{SM} \sim 7380$, while the background would be $\mathcal{N}_{Bg}^{SM} \sim 7080$, so that the *S.D.* number of the signal would be something like 3.6.

This fast fall-off of the observability when the Higgs mass increases, can be understood from the behaviour of the m_H dependence of the quantity $Br(H \rightarrow \gamma\gamma)Br(H \rightarrow ZZ)/m_H^2$ controlling the size of the Higgs contribution; and from the rise of the $\sigma_{++}(\gamma\gamma \rightarrow ZZ)$ background cross section with the energy; (compare [8] and Figs.20a,b). For example, $Br(H \rightarrow \gamma\gamma)Br(H \rightarrow ZZ)/m_H^2$ decreases by a factor of 80 as m_H increases from 300 to 500 GeV (mainly due to the decrease of $Br(H \rightarrow \gamma\gamma)$), while the background cross section increases by a factor 2 for the corresponding energy rise; compare *e.g.* [12, 2]. These two effects explain the strong decrease of the *S.D.* number as the Higgs mass increases.

As an application to SUSY, we investigate models in which all soft SUSY breaking sfermion mass parameters are taken at the TeV scale and the stop mixing maximal [22]. Such models have the tendency to push the mass of the CP even h^0 towards its highest possible values [23]. Thus, for a sufficiently heavy CP-odd A^0 Higgs particle and a not very small $\tan\beta$, they should be well within the presently allowed region [1, 24, 21]. Assuming also the gaugino unification condition

$$M_1 = \frac{5}{3} \tan^2 \theta_W M_2 \quad ,$$

we present in the first three lines of Table 1 six Sets of values for the independent parameters μ , M_2 , $M_{\tilde{f}}$, $\tan\beta$ and A_t . Taking also the mass m_{A^0} of the CP-odd A^0 as a further independent parameter, we show in the same table the implied stop, chargino and Higgs masses, as well as the Higgs widths and branching ratios calculated using HDECAY [23]. We have investigated cases where m_{A^0} is either 200 or 300 GeV, which imply similar (but somewhat higher masses) for the CP-even H^0 . In all these cases, the H^0 width is of the order of 0.1 to 0.2 GeV.

The resulting $\sigma_{++}(\gamma\gamma \rightarrow ZZ)$ cross sections around the narrow H^0 -pole for the Sets 3,4 of Table 1 are presented in Figs.3a,b respectively. Analogous results appear also for the cases of the other Sets of Table 1. As in the SM case, the numbers of signal and background events are determined using (18, 19), while the S.D. number is defined as in (22). These are given in the last three lines of Table 1, for all six sets of parameters considered.

As we see in Table 1, the number of standard deviations S.D. of the signal is largest in the lower side of $\tan\beta$ and A^0 masses considered (*i.e.* for $\tan\beta \simeq 3$ and $m_{A^0} \simeq 200\text{GeV}$). But as either $\tan\beta$ or m_{A^0} increase, S.D. is diminishing rather quickly. For $m_{A^0} = 200$ GeV, it is still sizable even for $\tan\beta = 7$; but for $m_{A^0} = 300$ GeV, the effect is visible only up to $\tan\beta \simeq 4$.

In order to understand the observability behaviour of the above SUSY cases, one should not only consider, as in the SM case, the quantity $Br(H \rightarrow \gamma\gamma)Br(H \rightarrow ZZ)/m_H^2$ and the energy rise of the background cross section $\sigma_{++}(\gamma\gamma \rightarrow ZZ)$, but also the fact that the H^0 is narrow, its width being much smaller than the photon-photon energy spread ($\Delta \simeq 10$ GeV). This last effect leads to a reduction of the signal by a factor (Γ_{H^0}/Δ) ; (in the SM case this effect does not occur for $m_H \gtrsim 300$ GeV, because $\Gamma_H \gtrsim 10$ GeV). Using then the Γ_H results given in Table 1, one can easily understand the values of the corresponding *S.D.* numbers.

We next briefly comment on the interference pattern between the H^0 -pole and the background contribution in the SUSY case. Such an effect would be evident in Fig.3b, which corresponds to $m_{H^0} = 300$ GeV and $\Gamma_{H^0} = 0.234$ GeV, provided that the energy resolution were perfect. But no interference pattern is obvious in the $m_{H^0} = 200$ GeV case of Fig.3a. Of course, with an energy resolution of about 10 GeV (as we have assumed in our analysis) it is not possible to observe interference patterns of the type of Fig.3b, by just averaging the data symmetrically around the Higgs mass. Nevertheless, it is important to remember that they might exist and to search for them by trying various selections of the binning, while analyzing experimental data. Since it may turn out that selections might exist which could appreciably modify the number of signal events, (say *e.g.* by selecting events mainly on one side of the resonance we are searching for) and thus help revealing a Higgs effect.

4 Conclusions

Assuming that the $\gamma\gamma$ Collider will be realized some day by applying the laser backscattering idea to an e^+e^- or e^-e^- LC, we have studied the observability of a standard or SUSY heavy neutral Higgs boson produced in the s -channel through $\gamma\gamma \rightarrow H^0 \rightarrow ZZ$. One of the motivations for performing this work was to investigate whether we could exploit the striking predominance of the helicity conserving purely imaginary amplitudes expected for the background $\gamma\gamma \rightarrow ZZ$ process at sufficiently high energies.

We have considered both, the case of the SM Higgs boson, as well as cases for the heavier CP-even H^0 Higgs predicted in MSSM. Under such circumstances, we have computed

Table 1: SUSY Sets of parameters at the electroweak scale.
(Dimensional quantities in GeV)

$M_2 = 200$, $\mu = 300$, $M_{\tilde{f}} = 1000$						
$\tan\beta$	3		4		5	7
$A_t = A_b = A_\tau$	2550		2600		2550	2550
$m_{\tilde{t}_1}$	785		777		781	779
$m_{\tilde{t}_2}$	1198		1204		1201	1202
$m_{\tilde{\chi}_1}$	165		168		170	173
$m_{\tilde{\chi}_2}$	340		339		337	336
m_{A^0}	200	300	200	300	200	200
m_{H^\pm}	214	310	215	310	215	215
m_{h^0}	109	113	115	118	119	122
m_{H^0}	212	307	207	304	205	203
Γ_{H^0}	0.105	0.240	0.112	0.234	0.135	0.216
$Br(H^0 \rightarrow ZZ)$	0.188	0.069	0.123	0.0475	0.0747	0.0263
$Br(H^0 \rightarrow \gamma\gamma) \times 10^5$	1.61	1.47	1.17	1.12	0.769	0.315
\mathcal{N}	804	403	468	342	231	57.6
\mathcal{N}_{Bg}	34	319	25.3	310	21.2	17.5
S.D.	132	4.7	88.6	1.8	45	9.5
	Set1	Set2	Set3	Set4	Set5	Set6

the amplitude for $\gamma\gamma \rightarrow H^0 \rightarrow ZZ$ in which the $\gamma\gamma \rightarrow H^0$ coupling arises at one-loop, while $H^0 \rightarrow ZZ$ exists at tree level; as well as the background $\gamma\gamma \rightarrow ZZ$ contribution arising through one-loop box amplitudes. In Section 2 and the Appendix, we have collected the explicit analytic expressions for the Higgs-pole and background amplitudes in the SM and the MSSM cases. They are presented in terms of Passarino-Veltman functions immediately suitable for computation. For most of the formulae we refer to [6, 7, 8], except for the mixed chargino box contributions arising from two different charginos running along the box diagram, which appear here for the first time.

We have then studied the interplay of the resonant Higgs contribution with the predominantly helicity conserving and imaginary background amplitude at sufficiently high energy. Depending on the parameters of the model, remarkable interference effects may appear, which in some cases enhance the Higgs signal.

Our first application has been to the standard Higgs search. We find that for masses in the region ($m_H \simeq 200 - 300$ GeV), the narrow Higgs peak largely dominates the background, and the interference effect does not play an important role. For higher masses (300 – 450 GeV) however, the constructive interference between the large imaginary parts of the Higgs and of the background amplitudes, increases the size of the Higgs peak. Even at higher masses (see the illustration at $m_H \simeq 500$ GeV in Fig.2b) this interference

pattern plays an important role for the Higgs detection. Therefore, the measurement of $\sigma_{++}(\gamma\gamma \rightarrow ZZ)$ constitutes a useful tool of the standard Higgs search, for Higgs masses in the range ($m_H \simeq 2m_Z - 500$ GeV). For even higher Higgs masses though, the strongly decreasing $Br(H \rightarrow \gamma\gamma)$ branching ratio prohibits an observable effect.

We have then considered the effects of the heavier CP-even H^0 predicted in MSSM. We have investigated part of the MSSM parameter space in which all sfermion SUSY breaking masses and their mixing are taken sufficiently large to guarantee an m_{h^0} value well within the presently allowed region; compare Table 1. The corresponding H^0 boson differs from an SM Higgs boson, by having a much narrower width and a smaller branching ratio to ZZ . Consequently the observability limit decreases to about $m_{H^0} \sim 300$ GeV for $\tan\beta \lesssim 4$; while for $\tan\beta \simeq 7$ it goes down to almost 200 GeV; see Table 1. In these computations we have of course taken into account the SUSY box contributions to $\gamma\gamma \rightarrow ZZ$ background.

We should also remark on the basis of the various numerical investigations performed, that the interference pattern between the Higgs-pole and background contributions varies, depending on the values of the SUSY parameters used. Examples of such an effect may be seen in Figs.3a,b. This is similar to what has also been observed in the SM case above. For comparisons, we have included in all figures the results expected in the SM case for $m_H = 100$ GeV.

In conclusion we can say that an experimental investigation of the $\gamma\gamma \rightarrow ZZ$ process and an analysis taking into account the interference between the Higgs resonance and the one loop background amplitudes, should be helpful for the identification of a scalar Higgs-like candidate.

Acknowledgments.

We are pleased to thank Abdelhak Djouadi for very useful and informative discussions about the SUSY Higgs properties. One of us (GJG) would also like to thank the CERN Theory Division for the hospitality extended to him while part of this work was performed.

Appendix: The $\gamma\gamma \rightarrow ZZ$ amplitudes in the Standard and SUSY models.

The invariant helicity amplitudes for the process

$$\gamma(p_1, \lambda_1)\gamma(p_2, \lambda_2) \rightarrow Z(p_3, \lambda_3)Z(p_4, \lambda_4) \quad , \quad (\text{A.1})$$

are denoted as⁶ $F_{\lambda_1\lambda_2\lambda_3\lambda_4}(\beta_Z, t, u)$, where the momenta and helicities of the incoming photons and outgoing Z 's are indicated in parentheses, and

$$s = (p_1 + p_2)^2 = \frac{4m_Z^2}{1 - \beta_Z^2} \quad , \quad t = (p_1 - p_3)^2 \quad , \quad u = (p_1 - p_4)^2 \quad , \quad (\text{A.2})$$

$$s_4 = s - 4m_Z^2 \quad , \quad s_2 = s - 2m_Z^2 \quad , \quad t_1 = t - m_Z^2 \quad , \quad u_1 = u - m_Z^2 \quad (\text{A.3})$$

are used. Denoting by ϑ^* the c.m. scattering angle of $\gamma\gamma \rightarrow ZZ$, we also note

$$t = m_Z^2 - \frac{s}{2}(1 - \beta_Z \cos \vartheta^*) \quad , \quad u = m_Z^2 - \frac{s}{2}(1 + \beta_Z \cos \vartheta^*) \quad , \quad (\text{A.4})$$

$$Y = tu - m_Z^4 = \frac{s^2\beta_Z^2}{4}\sin^2 \vartheta^* = sp_{TZ}^2 \quad , \quad \Delta = \sqrt{\frac{sm_Z^2}{2Y}} \quad , \quad (\text{A.5})$$

where p_{TZ} is the Z transverse momentum.

The parameter β_Z in (A.2) coincides with the Z -velocity in the ZZ c.m. frame. As in [7, 6, 8] it is used instead of s . The standard form of the Z polarization vectors implies the useful relation

$$F_{\lambda_1\lambda_2\lambda_3\lambda_4}(\beta_Z, t, u) = F_{\lambda_1\lambda_2, -\lambda_3, -\lambda_4}(-\beta_Z, t, u)(-1)^{\lambda_3 - \lambda_4} \quad , \quad (\text{A.6})$$

among the various helicity amplitudes. In addition, Bose statistics, combined with the Jacob-Wick (JW) [25] phase conventions demands

$$F_{\lambda_1\lambda_2\lambda_3\lambda_4}(\beta_Z, t, u) = F_{\lambda_2\lambda_1\lambda_4\lambda_3}(\beta_Z, t, u)(-1)^{\lambda_3 - \lambda_4} \quad , \quad (\text{A.7})$$

$$F_{\lambda_1\lambda_2\lambda_3\lambda_4}(\beta_Z, t, u) = F_{\lambda_2\lambda_1\lambda_3\lambda_4}(\beta_Z, u, t)(-1)^{\lambda_3 - \lambda_4} \quad , \quad (\text{A.8})$$

$$F_{\lambda_1\lambda_2\lambda_3\lambda_4}(\beta_Z, t, u) = F_{\lambda_1\lambda_2\lambda_4\lambda_3}(\beta_Z, u, t) \quad . \quad (\text{A.9})$$

while CP invariance, being equivalent to parity invariance at the 1-loop level, implies⁷

$$F_{\lambda_1\lambda_2\lambda_3\lambda_4}(\beta_Z, t, u) = F_{-\lambda_1, -\lambda_2, -\lambda_3, -\lambda_4}(\beta_Z, t, u)(-1)^{\lambda_3 - \lambda_4} \quad . \quad (\text{A.10})$$

Using (A.6) we remark that

$$F_{++--}(\beta_Z, t, u) = F_{++++}(-\beta_Z, t, u) \quad , \quad (\text{A.11})$$

$$F_{++-0}(\beta_Z, t, u) = -F_{+++0}(-\beta_Z, t, u) \quad , \quad (\text{A.12})$$

⁶The same definitions as in [8] are used.

⁷A sign error in Eqs.(A.13) of [8] is corrected in (A.12) here.

which combined with ($t \leftrightarrow u$) or helicity changes and the use of (A.7-A.10), allow to express the 36 $\gamma\gamma \rightarrow ZZ$ helicity amplitudes in terms of just the eight independent ones [8, 7, 6]

$$\begin{aligned} &F_{++++}(\beta_Z, t, u) , \ F_{++++}(\beta_Z, t, u), \ F_{+--+}(\beta_Z, t, u) , \ F_{+-00}(\beta_Z, t, u) , \\ &F_{++00}(\beta_Z, t, u) , \ F_{++++}(\beta_Z, t, u), \ F_{+-+0}(\beta_Z, t, u) , \ F_{+--+}(\beta_Z, t, u) . \end{aligned} \quad (\text{A.13})$$

In the non-linear gauge of [15] that we are using here, there are only two types of contributions to these amplitudes, in either the SM or SUSY models; see Fig.1. The first consists of the one-particle irreducible one-loop diagrams involving four external legs, similar to those contributing to the $\gamma\gamma \rightarrow \gamma\gamma$ and $\gamma\gamma \rightarrow \gamma Z$ processes [9, 10, 7]. We depict the generic form of these diagrams in Fig.1a and call them "boxes". Their contributions are given in this Appendix. The second type (discussed in Section 2) are one-particle reducible diagrams containing a Higgs s-channel pole and involving an⁸ $h^0\gamma\gamma$ vertex subdiagram [7]; see Fig1b.

The scalar boxes.

Such contributions are generated in MSSM through the effective Lagrangian

$$\mathcal{L}_{V\bar{S}S} = -ie(Q_S A^\mu + g_S^Z Z^\mu)(S^* \overleftrightarrow{\partial}_\mu S) + e^2(Q_S A^\mu + g_S^Z Z^\mu)^2 |S|^2 , \quad (\text{A.14})$$

where S is any scalar field. In the minimal SUSY case where $S = \tilde{t}_L, \tilde{t}_R, \tilde{b}_L, \tilde{b}_R, \tilde{\tau}_L, \tilde{\tau}_R, \tilde{\nu}_L$, or ⁹ H^+ , the corresponding coupling is

$$g_S^Z = \frac{1}{s_W c_W} (t_3^S - Q_S s_W^2) , \quad (\text{A.15})$$

in which t_3^S denotes the third isospin component of S .

The contribution to $\gamma\gamma \rightarrow ZZ$ of any such scalar particle is [8]

$$F_{\lambda_1 \lambda_2 \lambda_3 \lambda_4}^S(\beta_Z, t, u) \equiv \alpha^2 Q_S^2 N_S^c (g_S^Z)^2 A_{\lambda_1 \lambda_2 \lambda_3 \lambda_4}^S(\beta_Z, t, u; m) , \quad (\text{A.16})$$

where N_S^c counts the colour multiplicity of S , and $A_{\lambda_1 \lambda_2 \lambda_3 \lambda_4}^S$ is given by (A.34-A.41) in [8].

In cases like $\tilde{t}_{1,2}$, the non-diagonal mass matrix

$$\begin{pmatrix} \tilde{t}_L \\ \tilde{t}_R \end{pmatrix} = \begin{pmatrix} \cos \theta_t & -\sin \theta_t \text{Sign}(A_t - \mu \cot \beta) \\ \sin \theta_t \text{Sign}(A_t - \mu \cot \beta) & \cos \theta_t \end{pmatrix} \begin{pmatrix} \tilde{t}_1 \\ \tilde{t}_2 \end{pmatrix} , \quad (\text{A.17})$$

implies that the mixing angle always satisfies

$$\frac{\pi}{2} < \theta_t < \pi , \quad (\text{A.18})$$

⁸Here h^0 denotes any neutral Higgs boson.

⁹For H^+ we have $t_3^{H^+} = 1/2$ and $Q_{H^+} = 1$.

and it is fully determined by

$$\sin(2\theta_t) = \frac{2m_t|A_t - \mu \cot \beta|}{m_{\tilde{t}_1}^2 - m_{\tilde{t}_2}^2} \quad , \quad (\text{A.19})$$

provided we define $m_{\tilde{t}_1} < m_{\tilde{t}_2}$, and A_t is real.

Then, the single \tilde{t}_1 -box contribution is given by (A.16) for

$$g_{\tilde{t}_1}^Z = \frac{1}{s_W c_W} \left[\frac{1}{2} \cos^2 \theta_t - \frac{2s_W^2}{3} \right] \quad , \quad (\text{A.20})$$

while for the single \tilde{t}_2 one

$$g_{\tilde{t}_2}^Z = \frac{1}{s_W c_W} \left[\frac{1}{2} \sin^2 \theta_t - \frac{2s_W^2}{3} \right] \quad (\text{A.21})$$

should be used. In principle, we should also consider the mixed box contribution arising when both \tilde{t}_1 and \tilde{t}_2 are running along the box sides. Since such mixed contributions are expected to be at most of similar magnitude to the one coming from the single \tilde{t}_1 -box [27], which is already known to be extremely small [8], we have not calculated them.

If $\tan \beta \gtrsim 10$, then the \tilde{b}_1 -squark or $\tilde{\tau}_1$ -slepton contributions may be of similar magnitude. If desired, they may be directly obtained from (A.16) using the appropriate mixing matrix. Since in the numerical examples we consider these (as well as \tilde{t}_2) are very heavy, we refrain from giving their explicit contributions.

The W -boxes.

These are 1-loop diagrams involving four external legs, with a W , Goldstone or FP-ghost running along the loop. They have first been presented by [7]. We write them as

$$F_{\lambda_1 \lambda_2 \lambda_3 \lambda_4}^W(\beta_Z, t, u) \equiv \frac{\alpha^2}{s_W^2} A_{\lambda_1 \lambda_2 \lambda_3 \lambda_4}^W(\beta_Z, t, u) \quad , \quad (\text{A.22})$$

with $A_{\lambda_1 \lambda_2 \lambda_3 \lambda_4}^W$ given in (A.42-A.51) of [8].

The fermion boxes.

If the effective $(\gamma, Z)f\bar{f}$ interaction is written as

$$\mathcal{L}_{Vff} = -eA^\mu \bar{f} \gamma_\mu f - eZ^\mu \bar{f} (\gamma_\mu g_{vf}^Z - \gamma_\mu \gamma_5 g_{af}^Z) f \quad , \quad (\text{A.23})$$

then the fermion loop contribution to the $\gamma\gamma \rightarrow ZZ$ helicity amplitude for a fermion of mass m_f , is given by [6, 8]

$$F_{\lambda_1 \lambda_2 \lambda_3 \lambda_4}^f(\beta_Z, t, u) \equiv \alpha^2 Q_f^2 N_f^c \left\{ (g_{vf}^Z)^2 A_{\lambda_1 \lambda_2 \lambda_3 \lambda_4}^{vf}(\beta_Z, t, u; m_f) + (g_{af}^Z)^2 A_{\lambda_1 \lambda_2 \lambda_3 \lambda_4}^{af}(\beta_Z, t, u; m_f) \right\} \quad , \quad (\text{A.24})$$

where N_f^c counts the colour multiplicity and A^{vf} , A^{af} are given by (A.55-A.71) of [8].

For quarks and leptons

$$g_{vf}^Z = \frac{t_3^f - 2Q_f s_W^2}{2s_W c_W} \quad , \quad g_{af}^Z = \frac{t_3^f}{2s_W c_W} \quad , \quad (\text{A.25})$$

where t_3^f is the third isospin component of the fermion, and Q_f is its charge.

The specific case of a chargino fermion requires a more extensive discussion, because of their possible mixed coupling to Z . The relevant parameters are determined by the mass matrix

$$\mathcal{L}_{M_\chi} = -(\tilde{W}^{-\tau}, \tilde{H}_1^{-\tau})_L \cdot C \cdot \begin{pmatrix} M_2 & \sqrt{2}m_W \sin \beta \\ \sqrt{2}m_W \cos \beta & +\mu \end{pmatrix} \begin{pmatrix} \tilde{W}^+ \\ \tilde{H}_2^+ \end{pmatrix}_L + \text{h.c.} \quad , \quad (\text{A.26})$$

leading to the physical chargino masses

$$m_{\tilde{\chi}_1, \tilde{\chi}_2} = \frac{1}{\sqrt{2}}[M_2^2 + \mu^2 + 2m_W^2 \mp \tilde{D}]^{1/2} \quad , \quad (\text{A.27})$$

where

$$\tilde{D} \equiv [(M_2^2 + \mu^2 + 2m_W^2)^2 - 4(M_2\mu - m_W^2 \sin(2\beta))^2]^{1/2} \quad , \quad (\text{A.28})$$

for any sign of M_2 , μ . Defining then the mixing-angles ϕ_R, ϕ_L as [26]

$$\begin{aligned} \cos \phi_L &= -\frac{1}{\sqrt{2\tilde{D}}}[\tilde{D} - M_2^2 + \mu^2 + 2m_W^2 \cos 2\beta]^{1/2} \quad , \\ \cos \phi_R &= -\frac{1}{\sqrt{2\tilde{D}}}[\tilde{D} - M_2^2 + \mu^2 - 2m_W^2 \cos 2\beta]^{1/2} \quad , \end{aligned} \quad (\text{A.29})$$

so that they always lie in the second quarter

$$\frac{\pi}{2} \leq \phi_L < \pi \quad , \quad \frac{\pi}{2} \leq \phi_R < \pi \quad ; \quad (\text{A.30})$$

the effective Lagrangian for the (γ, Z) -chargino interaction becomes¹⁰

$$\begin{aligned} \mathcal{L} &= -eA^\mu \bar{\tilde{\chi}}_j \gamma_\mu \tilde{\chi}_j - eZ^\mu \bar{\tilde{\chi}}_j (\gamma_\mu g_{vj} - \gamma_\mu \gamma_5 g_{aj}) \tilde{\chi}_j \\ &\quad - eZ^\mu [\bar{\tilde{\chi}}_1 (\gamma_\mu g_{v12} - \gamma_\mu \gamma_5 g_{a12}) \tilde{\chi}_2 + \text{h.c.}] \quad , \end{aligned} \quad (\text{A.31})$$

where

$$\begin{aligned} g_{v1} &= \frac{1}{2s_W c_W} \left(\frac{3}{2} - 2s_W^2 + \frac{1}{4}[\cos 2\phi_L + \cos 2\phi_R] \right) \quad , \\ g_{a1} &= -\frac{1}{8s_W c_W} [\cos 2\phi_L - \cos 2\phi_R] \quad , \end{aligned} \quad (\text{A.32})$$

¹⁰The chargino field is always defined so that it absorbs a positive chargino particle; *i.e.* $\tilde{\chi}_j \equiv \tilde{\chi}_j^+$ ($j = 1, 2$).

$$\begin{aligned}
g_{v2} &= \frac{1}{2s_W c_W} \left(\frac{3}{2} - 2s_W^2 - \frac{1}{4} [\cos 2\phi_L + \cos 2\phi_R] \right) , \\
g_{a2} &= \frac{1}{8s_W c_W} [\cos 2\phi_L - \cos 2\phi_R] ,
\end{aligned} \tag{A.33}$$

$$\begin{aligned}
g_{v12} &= -\frac{\text{Sign}(M_2)}{8s_W c_W} [\tilde{\mathcal{B}}_R \tilde{\Delta}_{12} \sin 2\phi_R + \tilde{\mathcal{B}}_L \sin 2\phi_L] , \\
g_{a12} &= -\frac{\text{Sign}(M_2)}{8s_W c_W} [\tilde{\mathcal{B}}_R \tilde{\Delta}_{12} \sin 2\phi_R - \tilde{\mathcal{B}}_L \sin 2\phi_L] .
\end{aligned} \tag{A.34}$$

The box-contribution from the single chargino couplings in (A.32, A.33) are given by the same expressions (A.24). But for charginos we also have the "mixed" $Z\tilde{\chi}_1\tilde{\chi}_2$ -couplings appearing in (A.34), which generate boxes with two different charginos running along the loop. These couplings, as well as those of the neutral Higgs to charginos defined in Section 2, depend on the sign-quantities

$$\begin{aligned}
\tilde{\mathcal{B}}_L &= \text{Sign}(\mu \sin \beta + M_2 \cos \beta) , \\
\tilde{\mathcal{B}}_R &= \text{Sign}(\mu \cos \beta + M_2 \sin \beta) , \\
\tilde{\mathcal{B}}_{LR} &\equiv \text{Sign} \left(M_2 \mu + \frac{\mu^2 + M_2^2}{2} \sin 2\beta \right) = \tilde{\mathcal{B}}_L \tilde{\mathcal{B}}_R , \\
\tilde{\Delta}_1 &= \text{Sign}(M_2 [\tilde{D} - M_2^2 + \mu^2 - 2m_W^2] - 2m_W^2 \mu \sin 2\beta) , \\
\tilde{\Delta}_2 &= \text{Sign}(\mu [\tilde{D} - M_2^2 + \mu^2 + 2m_W^2] + 2m_W^2 M_2 \sin 2\beta) , \\
\tilde{\Delta}_{12} &\equiv \text{Sign}(M_2 \mu - m_W^2 \sin 2\beta) = \tilde{\Delta}_1 \tilde{\Delta}_2 ,
\end{aligned} \tag{A.35}$$

constructed to guarantee the positivity of the physical chargino masses and the usual relation between the fields absorbing the positive and negative charginos; *i.e.* $C\tilde{\chi}^{+\tau} = \tilde{\chi}^-$ [26].

The mixed chargino boxes.

This contribution, generated by the $Z\tilde{\chi}_1\tilde{\chi}_2$ - couplings in (A.34), is denoted as¹¹

$$\begin{aligned}
F_{\lambda_1 \lambda_2 \lambda_3 \lambda_4}^{\tilde{\chi}_1 \tilde{\chi}_2}(\beta_Z, t, u) &\equiv \alpha^2 [(g_{v12})^2 + (g_{a12})^2] (-1)^{1-\lambda_4} A_{\lambda_1 \lambda_2 \lambda_3 \lambda_4}^{(\tilde{\chi}_1 \tilde{\chi}_2 1)}(\beta_Z, t, u; m_{\tilde{\chi}_1^2}, m_{\tilde{\chi}_2^2}) \\
&+ \alpha^2 [(g_{v12})^2 - (g_{a12})^2] m_{\tilde{\chi}_1} m_{\tilde{\chi}_2} (-1)^{1-\lambda_4} A_{\lambda_1 \lambda_2 \lambda_3 \lambda_4}^{(\tilde{\chi}_1 \tilde{\chi}_2 2)}(\beta_Z, t, u; m_{\tilde{\chi}_1^2}, m_{\tilde{\chi}_2^2}) .
\end{aligned} \tag{A.36}$$

The form of (A.36) is motivated by the fact that the structure of the mixed boxes allow only the existence of either g_{v12}^2 or g_{a12}^2 terms, which are related to each other through the substitutions:

$$g_{v12} \leftrightarrow g_{a12} \quad \text{and} \quad (m_1, m_2) \leftrightarrow (-m_1, m_2) .$$

To describe this mixed chargino contribution, we need the Passarino-Veltman functions [16], for which we follow the notation of [17] and the abbreviations¹²

$$B_Z^{11}(s) \equiv B_0(s; m_1, m_1) - B_0(m_Z^2 + i\epsilon; m_1, m_2) , \tag{A.37}$$

¹¹The factor $(-1)^{1-\lambda_4}$ comes from the JW helicity convention [25].

¹²In the middle terms of (A.40-A.46) $k_1 = p_1$, $k_2 = p_2$ denote the momenta of the photons, while $k_3 = -p_3$, $k_4 = -p_4$ those of the A^0 , always taken as incoming; compare (A.1).

$$B_Z^{22}(s) \equiv B_0(s; m_2, m_2) - B_0(m_Z^2 + i\epsilon; m_1, m_2) , \quad (\text{A.38})$$

$$B_Z^{12}(s) \equiv B_0(s; m_1, m_2) - B_0(m_Z^2 + i\epsilon; m_1, m_2) , \quad (\text{A.39})$$

$$C_0^{abc}(s) \equiv C_0(k_1, k_2) = C_0(0, 0, s; m_a, m_b, m_c) , \quad (\text{A.40})$$

$$C_Z^{abc}(u) \equiv C_0(k_3, k_2) = C_0(m_Z^2, 0, u; m_a, m_b, m_c) , \quad (\text{A.41})$$

$$C_{ZZ}^{abc}(s) \equiv C_0(k_3, k_4) = C_0(m_Z^2, m_Z^2, s; m_a, m_b, m_c) , \quad (\text{A.42})$$

$$D_{ZZ}^{abcd}(s, t) \equiv D_0(k_4, k_3, k_1) = D_0(m_Z^2, m_Z^2, 0, 0, s, t; m_a, m_b, m_c, m_d) , \quad (\text{A.43})$$

$$D_{ZZ}^{abcd}(s, u) \equiv D_0(k_3, k_4, k_1) = D_0(m_Z^2, m_Z^2, 0, 0, s, u; m_a, m_b, m_c, m_d) , \quad (\text{A.44})$$

$$D_{ZZ}^{abcd}(t, u) \equiv D_0(k_3, k_1, k_4) = D_0(m_Z^2, 0, m_Z^2, 0, t, u; m_a, m_b, m_c, m_d) , \quad (\text{A.45})$$

$$D_{ZZ}^{abcd}(u, t) \equiv D_0(k_4, k_1, k_3) = D_0(m_Z^2, 0, m_Z^2, 0, u, t; m_a, m_b, m_c, m_d) , \quad (\text{A.46})$$

$$\tilde{F}^{ab}(s, t, u) = D_{ZZ}^{abba}(t, u) + D_{ZZ}^{abaa}(s, t) + D_{ZZ}^{abaa}(s, u) , \quad (\text{A.47})$$

$$E_1^{ab}(s, u) = 2u_1 C_Z^{baa}(u) - su D_{ZZ}^{abaa}(s, u) , \quad (\text{A.48})$$

$$\begin{aligned} E_2^{ab}(t, u) &= t_1 [C_Z^{abb}(t) + C_Z^{baa}(t)] + u_1 [C_Z^{abb}(u) + C_Z^{baa}(u)] \\ &\quad - Y D_{ZZ}^{abba}(t, u) , \end{aligned} \quad (\text{A.49})$$

which are closely related to those in¹³ Eqs.(A.14 - A.24) of [8].

We also note that

$$\begin{aligned} D_{ZZ}^{abba}(t, u) &= D_{ZZ}^{abba}(u, t) = D_{ZZ}^{baab}(t, u) = D_{ZZ}^{baab}(u, t) , \\ \tilde{F}^{ab}(s, t, u) &= \tilde{F}^{ab}(s, u, t) , \quad E_2^{ab}(t, u) = E_2^{ab}(u, t) = E_2^{ba}(t, u) . \end{aligned} \quad (\text{A.50})$$

Thus, the eight basic amplitudes listed in (A.13, A.36) are determined by¹⁴

$$\begin{aligned} A_{++++}^{(\tilde{\chi}_1 \tilde{\chi}_2 1)}(\beta_Z, t, u; m_1^2, m_2^2) &= -\frac{16[m_Z^2(2Y - ss_4) + \beta_Z s Y]}{s_4 t_1 u_1} \\ &+ \frac{4(s_2 + s\beta_Z)}{s_4 s} \left[\frac{(2Y - ss_4)}{s} E_2^{12}(t, u) + \frac{4m_Z^2 Y + 2t_1(2t_1 + s)(t + m_Z^2)}{t_1^2} B_Z^{12}(t) \right. \\ &\quad \left. + \frac{4m_Z^2 Y + 2u_1(2u_1 + s)(u + m_Z^2)}{u_1^2} B_Z^{12}(u) \right] \\ &+ \frac{8}{s_4} \left\{ -2m_1^2[2(m_Z^2 + m_2^2 - m_1^2) + s\beta_Z] C_0^{111}(s) + \frac{(m_1^2 - m_2^2)^2}{s} [E_2^{12}(t, u) \right. \\ &\quad \left. - 2sm_1^2 \tilde{F}^{12}(s, t, u)] - \frac{(m_1^2 + m_2^2)(2Y - ss_4)(s_2 + \beta_Z s)}{4s} D_{ZZ}^{1221}(t, u) \right. \\ &\quad \left. - 2m_1^2 m_Z^2 (s_2 + \beta_Z s) \left[\frac{1}{u_1} C_Z^{211}(u) + \frac{1}{t_1} C_Z^{211}(t) \right] + m_1^2 [s(m_1^2 - m_2^2) \right. \\ &\quad \left. - s_2 m_Z^2 - \beta_Z s(m_Z^2 + m_2^2 - m_1^2)] [D_{ZZ}^{1211}(s, u) + D_{ZZ}^{1211}(s, t)] + (1 \leftrightarrow 2) \right\} , \end{aligned} \quad (\text{A.51})$$

¹³Notice that the present definition of E_1 differs somewhat from the one employed in [26], where an analogous mixed case is also treated.

¹⁴For brevity we identify here $m_j \equiv m_{\tilde{\chi}_j}$.

$$A_{++++}^{(\tilde{\chi}_1\tilde{\chi}_2^{22})}(\beta_Z, t, u; m_1^2, m_2^2) = \frac{8}{s_4} \left\{ 2\beta_Z s C_0^{111}(s) + \frac{s_4 + \beta_Z s}{s} E_2^{12}(t, u) - 2m_1^2 s_4 \tilde{F}^{12}(s, t, u) \right. \\ \left. + \frac{s}{2} [s_4 + \beta_Z (s_2 + 2m_2^2 - 2m_1^2)] [D_{ZZ}^{1211}(s, u) + D_{ZZ}^{1211}(s, t)] + (1 \leftrightarrow 2) \right\}, \quad (\text{A.52})$$

$$A_{+--+}^{(\tilde{\chi}_1\tilde{\chi}_2^{21})}(\beta_Z, t, u; m_1^2, m_2^2) = \frac{16s_2 Y}{s_4 t_1 u_1} - \frac{4m_Z^2 s (s_2^2 - 2Y)}{s_4 Y} [C_0^{111}(s) + C_0^{222}(s)] \\ + \frac{4m_Z^2 s_2 (2Y - ss_4)}{s_4 Y} [C_{ZZ}^{121}(s) + C_{ZZ}^{212}(s)] - \frac{4m_Z^2}{s_4} \left\{ \frac{4(Y + 2um_Z^2)}{u_1^2} B_Z^{12}(u) \right. \\ \left. + \frac{(u^2 + m_Z^4)}{Y} [E_1^{12}(s, u) + E_1^{21}(s, u)] + (u \leftrightarrow t) \right\} \\ + \frac{4}{s_4 Y} \left\{ s(m_1^2 - m_2^2) [4(m_1^2 - m_2^2)(m_Z^2 + m_1^2 - m_2^2 - s) + s_2(s + 2m_Z^2) - 2Y] C_0^{111}(s) \right. \\ - (2Y - ss_4)(m_1^2 - m_2^2) [s - 2(m_1^2 - m_2^2)] C_{ZZ}^{121}(s) - 2s(m_1^2 - m_2^2)^4 \tilde{F}^{12}(s, t, u) \\ - \left(2Y(m_1^4 - m_2^4)(m_1^2 - m_2^2) - (2Y - ss_4)m_Z^2 \left[(m_1^2 - m_2^2)^2 + \frac{(m_1^2 + m_2^2)Y}{s} \right] \right) D_{ZZ}^{1221}(t, u) \\ \left. + \left[\left(\frac{2u_1}{s} (m_1^2 - m_2^2) [u_1(2m_Z^4 - 3m_Z^2 s + us_2) - (m_1^2 - m_2^2)s(s - 2u)] - \frac{4m_1^2 s_2 Y^2}{su_1} \right) C_Z^{211}(u) \right. \right. \\ \left. - \left((m_1^6 - m_2^6)s(4u - s) - (m_1^2 - m_2^2)s(m_Z^6 - uu_1^2 + m_Z^2 tu + 2m_Z^2 u^2) \right. \right. \\ \left. + m_1^2 m_2^2 (m_1^2 - m_2^2)(8u_1^2 + 3s^2 - 4su) + (m_1^2 - m_2^2)^2 s(sm_Z^2 + 4uu_1) \right. \\ \left. \left. - (m_1^4 - m_2^4)sY + 2Ym_1^2[2(m_1^4 - m_2^4) + s_2 m_Z^2] \right) D_{ZZ}^{1211}(s, u) + (u \leftrightarrow t) \right] \\ \left. + (1 \leftrightarrow 2) \right\}, \quad (\text{A.53})$$

$$A_{+--+}^{(\tilde{\chi}_1\tilde{\chi}_2^{22})}(\beta_Z, t, u; m_1^2, m_2^2) = \frac{8}{Y} \left\{ s[2(m_1^2 - m_2^2) - s_2] C_0^{111}(s) + (2Y - ss_4) C_{ZZ}^{121}(s) \right. \\ \left. - s(m_1^2 - m_2^2)^2 \tilde{F}^{12}(s, t, u) - \frac{Y}{s_4} [s_4(m_1^2 + m_2^2) + Y] D_{ZZ}^{1221}(t, u) \right. \\ \left. + \left[uE_1^{12}(s, u) + 2(m_1^2 u_1^2 + m_2^2 su) D_{ZZ}^{1211}(s, u) + (u \leftrightarrow t) \right] + (1 \leftrightarrow 2) \right\}, \quad (\text{A.54})$$

$$A_{++++}^{(\tilde{\chi}_1\tilde{\chi}_2^{21})}(\beta_Z, t, u; m_1^2, m_2^2) = \frac{16Y}{s_4} \left[\frac{s_2}{t_1 u_1} - \frac{m_Z^2}{s^2} E_2^{12}(t, u) + \frac{m_Z^2}{t_1^2} \left(\frac{2t}{s} - 1 \right) B_Z^{12}(t) \right. \\ \left. + \frac{m_Z^2}{u_1^2} B_Z^{12}(u) \right] + \frac{8}{Y s_4} \left(-m_1^2 [2(m_1^2 - m_2^2) - s_2] (2Y - ss_4) C_0^{111}(s) - m_1^2 s s_4^2 C_{ZZ}^{121}(s) \right. \\ \left. + \frac{Y s_4}{2s} (m_1^2 + m_2^2) E_2^{12}(t, u) + m_1^2 (m_1^2 - m_2^2)^2 (2Y - ss_4) \tilde{F}^{12}(s, t, u) \right)$$

$$\begin{aligned}
& + \frac{Y}{s} \left[Y[m_Z^2(m_1^2 + m_2^2) - 2m_1^2 m_2^2] + (m_1^4 + m_2^4)(Y - ss_4) \right] D_{ZZ}^{1221}(t, u) \\
& + \left\{ \frac{1}{su_1} \left[-u_1^2(m_1^2 - m_2^2)^2(2Y - ss_4) + 2sm_1^2[2m_Z^4(Y + 2u^2) - u^2 s_2^2] \right] C_Z^{211}(u) \right. \\
& + m_1^2[-2(m_1^2 - m_2^2)(m_Z^4 t - 3m_Z^4 u - u^2 s_2) + 2Y(m_Z^4 - m_1^2 s_4) \\
& \left. + (4m_Z^4 - s_2^2)u^2] D_{ZZ}^{1211}(s, u) + (u \leftrightarrow t) \right\} + (1 \leftrightarrow 2) \Big) , \tag{A.55}
\end{aligned}$$

$$A_{++++}^{(\tilde{\chi}_1 \tilde{\chi}_2^2)}(\beta_Z, t, u; m_1^2, m_2^2) = 0 , \tag{A.56}$$

$$\begin{aligned}
A_{+-00}^{(\tilde{\chi}_1 \tilde{\chi}_2^1)}(\beta_Z, t, u; m_1^2, m_2^2) = & -\frac{64m_Z^2 Y}{s_4 t_1 u_1} + \frac{8sm_Z^2(s_2^2 - 2Y)}{s_4 Y} [C_0^{111}(s) + C_0^{222}(s)] \\
& - \frac{8m_Z^2 s_2(2Y - ss_4)}{s_4 Y} [C_{ZZ}^{121}(s) + C_{ZZ}^{212}(s)] + \left\{ \frac{8m_Z^2}{s_4 Y} (u^2 + m_Z^4) [E_1^{12}(s, u) + E_1^{21}(s, u)] \right. \\
& \left. - \frac{32m_Z^2(u^2 + m_Z^4)}{s_4 u_1^2} B_Z^{12}(u) + (u \leftrightarrow t) \right\} \\
& + \frac{2}{s_4 Y m_Z^2} \left[-s[4s(m_1^2 - m_2^2)^3 - 16m_1^2 m_Z^2(m_1^2 - m_2^2)(s - m_Z^2) \right. \\
& + 4m_2^2(m_1^2 - m_2^2)(4m_Z^4 + ss_2) + 4(m_1^2 - m_2^2)m_Z^2(4m_Z^2 s_2 + s_2^2 - 2Y) \\
& - (m_1^2 + m_2^2)s_4(s_2^2 - 2Y)] C_0^{111}(s) - (2Y - ss_4)[(m_1^2 + m_2^2)(s^2 + 8m_Z^4) + 2s(m_1^2 - m_2^2)^2 \\
& - 2m_Z^2 s(5m_1^2 + m_2^2)] C_{ZZ}^{121}(s) + \frac{1}{s} \left\{ 2s^3(m_1^2 - m_2^2)^4 + ss_2(s - 8m_Z^2)Y(m_1^4 + m_2^4) \right. \\
& + (m_1^2 - m_2^2)(m_1^4 - m_2^4)s^2(s_4 s_2 + 2Y) - 4m_Z^2 s_2 Y^2(m_1^2 + m_2^2) + 2m_1^2 m_2^2 s^2 s_2 Y \Big\} D_{ZZ}^{1221}(t, u) \\
& + \left\{ \frac{2}{su_1} \left[-2(m_1^2 - m_2^2)^2(u - 2m_Z^2)u_1^2 s^2 + 8m_1^2 sm_Z^2(m_Z^6 t + 5m_Z^6 u - 3m_Z^4 tu \right. \right. \\
& - 7m_Z^4 u^2 + m_Z^2 tu^2 + 5m_Z^2 u^3 - tu^3 - u^4) + (m_1^2 + m_2^2)u_1^2[8u_1^2 m_Z^4 + 5m_Z^4 ss_2 \\
& - 2m_Z^2 s(2us_2 + m_Z^4) + ss_4 u^2] \Big] C_Z^{211}(u) + \left\{ 2s^2(m_1^2 - m_2^2)^4 + m_2^6 s(s^2 - 2m_Z^2 s_4 - 4su) \right. \\
& - m_1^4 m_2^2 s(s^2 - 18sm_Z^2 + 16um_Z^2 + 4su - 8u^2) + m_1^6 s[8m_Z^4 + s(s - 10m_Z^2) - 4u_1^2] \\
& - m_1^2 m_2^4 s(28m_Z^4 - 10m_Z^2 t + t^2 - 34m_Z^2 u + 10tu + 13u^2) - (m_1^2 - m_2^2)^2 s(8m_Z^6 \\
& - 5m_Z^4 s + 16m_Z^4 u + ss_2 u - 3su^2) - 4m_1^4[4u_1^2 m_Z^4 + s(u^2 + m_Z^4)(s - 7m_Z^2) \\
& + sum_Z^2(10m_Z^2 - 3s)] - 4m_1^2 m_2^2[m_Z^2(s + 4m_Z^2)(u^2 + m_Z^4) - 8m_Z^6 u - 5m_Z^2 ss_2 u \\
& + s^3 u] - m_2^2 s(-4m_Z^8 - 8m_Z^6 u + 5m_Z^4 su - 12m_Z^4 u^2 + su^3) \\
& + m_1^2(16m_Z^6 u_1^2 - 12m_Z^8 s + 32m_Z^6 su - 5m_Z^4 s^2 u - 20m_Z^4 su^2 + 8m_Z^2 su^3 \\
& \left. \left. - s^2 u^3) \right\} D_{ZZ}^{1211}(s, u) + (u \leftrightarrow t) \right\} + (1 \leftrightarrow 2) \Big] , \tag{A.57}
\end{aligned}$$

$$A_{+-00}^{(\tilde{\chi}_1 \tilde{\chi}_2^2)}(\beta_Z, t, u; m_1^2, m_2^2) = \frac{2}{s_4 Y m_Z^2} \left[2s_4 s[2(m_1^2 - m_2^2)s_2 - s_2^2 + 2Y] C_0^{111}(s) \right.$$

$$\begin{aligned}
& -2(6m_Z^2s - 8m_Z^4 - s^2)(2Y - ss_4)C_{ZZ}^{121}(s) - 2[ss_2s_4(m_1^2 - m_2^2)^2 + s_4s_2Y(m_1^2 + m_2^2) \\
& - 4m_Z^2Y^2]D_{ZZ}^{1221}(t, u) - 2s_4\left\{(u^2 + m_Z^4)E_1^{12}(s, u) + [(m_1^2 - m_2^2)^2ss_2 + m_2^2s(2u^2 + tu + m_Z^4) \right. \\
& \left. + m_1^2(4m_Z^2u_1^2 - 3su_1^2 - s^2u)]D_{ZZ}^{1211}(s, u) + (u \leftrightarrow t)\right\} + (1 \leftrightarrow 2) \Big] , \tag{A.58}
\end{aligned}$$

$$\begin{aligned}
A_{+++0}^{(\tilde{\chi}_1\tilde{\chi}_2^{11})}(\beta_Z, t, u; m_1^2, m_2^2) = & \frac{8(1 + \beta_Z)Y}{s_4} \left[-\frac{2(t - u)}{t_1u_1} - \frac{2(m_Z^2s - 2uu_1)}{su_1^2}B_Z^{12}(u) \right. \\
& + \frac{2(m_Z^2s - 2tt_1)}{st_1^2}B_Z^{12}(t) + \frac{(t - u)}{s^2}E_2^{12}(t, u) \Big] + \frac{2}{s_4m_Z^2} \left[2m_1^2(t - u)[4(m_1^2 - m_2^2) \right. \\
& - (1 + \beta_Z)s]C_0^{111}(s) - \frac{(t - u)}{2s} \left\{ (m_1^2 - m_2^2)^2[4s(m_1^2 + m_2^2) - (t - u)^2] \right. \\
& + 4m_Z^2(m_1^2 + m_2^2)Y(1 + \beta_Z) + 4\beta_Zm_1^2m_2^2ss_4 - \beta_Z(m_1^2 + m_2^2)^2ss_4 \Big\} D_{ZZ}^{1221}(t, u) \\
& + \frac{s_4(u - t)(m_1^2 + m_2^2)(1 + \beta_Z)}{2s}E_2^{12}(t, u) + \left\{ \frac{4}{su_1}[-u_1^2(u - t)(m_1^2 - m_2^2)^2 \right. \\
& + 2(1 + \beta_Z)m_1^2m_Z^2s(m_Z^4 - Y - u^2)]C_Z^{211}(u) - m_1^2[4(m_1^2 - m_2^2) \\
& - (1 + \beta_Z)s][(m_1^2 - m_2^2)(t - u) + m_Z^4 - Y - u^2]D_{ZZ}^{1211}(s, u) - (u \leftrightarrow t) \Big\} \\
& \left. + (1 \leftrightarrow 2) \right] , \tag{A.59}
\end{aligned}$$

$$\begin{aligned}
A_{+++0}^{(\tilde{\chi}_1\tilde{\chi}_2^{22})}(\beta_Z, t, u; m_1^2, m_2^2) = & \frac{2(s_4 + \beta_Zs)}{s_4m_Z^2} \left[2(t - u)C_0^{111}(s) + \frac{(t - u)}{s}E_2^{12}(t, u) \right. \\
& + [(m_1^2 - m_2^2)(u - t) + m_Z^4 - Y - t^2]D_{ZZ}^{1211}(s, t) \\
& \left. - [(m_1^2 - m_2^2)(t - u) + m_Z^4 - Y - u^2]D_{ZZ}^{1211}(s, u) + (1 \leftrightarrow 2) \right] , \tag{A.60}
\end{aligned}$$

$$\begin{aligned}
A_{+-+0}^{(\tilde{\chi}_1\tilde{\chi}_2^{11})}(\beta_Z, t, u; m_1^2, m_2^2) = & -\frac{16Y(u - t - s\beta_Z)}{s_4t_1u_1} + \frac{8(u - t + s\beta_Z)}{s_4}[B_Z^{11}(s) + B_Z^{22}(s)] \\
& - \frac{4s}{s_4Y}[(t - u)(Y + u^2 + t^2) + \beta_Z(tt_1^2 + uu_1^2 - 2m_Z^2Y)][C_0^{111}(s) + C_0^{222}(s)] \\
& + \frac{4}{s_4Y}\{(u - t)s_4(t_1^2 + u_1^2 + Y) - \beta_Zs[tt_1(t + m_Z^2) + uu_1(u + m_Z^2) \\
& - 2m_Z^2Y]\}[C_{ZZ}^{121}(s) + C_{ZZ}^{212}(s)] + \left\{ \frac{16}{s_4u_1^2}[m_Z^2Y - uu_1(u + m_Z^2) - \beta_Z(m_Z^2Y - uu_1^2)]B_Z^{12}(u) \right. \\
& - \frac{4}{s_4Y}[m_Z^2Y - uu_1(u + m_Z^2) + \beta_Z(uu_1^2 - m_Z^2Y)][E_1^{12}(s, u) + E_1^{21}(s, u)] \\
& \left. - (u \leftrightarrow t \quad , \quad \beta_Z \rightarrow -\beta_Z) \right\} + \frac{2}{m_Z^2s_4Y} \left[-4Y(m_1^2 - m_2^2)(u - t + \beta_Zs)B_Z^{11}(s) \right.
\end{aligned}$$

$$\begin{aligned}
& +2\{(m_1^2 - m_2^2)(t - u)[2s(m_1^2 - m_2^2)(m_1^2 - m_2^2 + m_Z^2 - s) + s(Y + tt_1 + uu_1 + m_Z^2 s_2)] \\
& + m_1^2(t - u)s_4 Y - \beta_Z s[2s(m_1^2 - m_2^2)^3 + 2(m_1^4 + m_2^4)(m_Z^2 - s)s + 4m_1^4 Y + 4m_1^2 m_2^2(t_1^2 \\
& + u_1^2 + m_Z^2 s + Y) + (m_1^2 - m_2^2)(4m_Z^2 u_1^2 + s^2 s_2 + 2su(u + s)) - m_2^2 Y s]\} C_0^{111}(s) \\
& + 2(m_1^2 - m_2^2)s(s + 2m_2^2 - 2m_1^2)[u(u + 2m_Z^2) - t(t + 2m_Z^2) + \beta_Z(2Y - ss_4)] C_{ZZ}^{121}(s) \\
& - 2(m_1^2 - m_2^2)^4 s(t - u - \beta_Z s) \tilde{F}^{12}(s, t, u) - \frac{Y}{2} \{(t - u)[4(m_1^2 - m_2^2)(m_1^4 - m_2^4) \\
& - s(m_1^2 - m_2^2)^2 - Y(m_1^2 + m_2^2)] - \beta_Z[8s(m_1^2 - m_2^2)(m_1^4 - m_2^4) + (m_1^2 + m_2^2)Y s_4 \\
& + (m_1^2 - m_2^2)^2(ss_4 + 4Y)]\} D_{ZZ}^{1221}(t, u) + \left[-\frac{1}{u_1} \left\{ -4u_1^2(m_1^2 - m_2^2)^2(sm_Z^2 - 2uu_1) \right. \right. \\
& + u_1^2(m_1^2 - m_2^2)(8m_Z^6 + tY - 7m_Z^4 u - 8m_Z^2 u^2 + 3tu^2 + 4u^3) + 2m_1^2(u - t)(u + m_Z^2)^2 Y \\
& + \beta_Z \{4(m_1^2 - m_2^2)^2 u_1^3(s - u_1) + (m_1^2 - m_2^2)u_1^2[4m_Z^2 u_1^2 - s(u + m_Z^2)^2 + su(4u - s)] \\
& - 2m_1^2 Y[4m_Z^2 u_1^2 + s(u + m_Z^2)^2]\} \} C_Z^{211}(u) + \left\{ -2su_1(s + 4u)(m_2^6 - m_1^6 - m_1^4 m_2^2 \right. \\
& - m_1^2 m_2^4) - 4Ym_1^6(t - u) - 4m_1^2 m_2^2(2m_1^2 - m_2^2)(s - 2u_1)(m_Z^2 t_1 + uu_1) \\
& + (m_1^2 - m_2^2)^2 s(4m_Z^6 + tY - 7m_Z^4 u + 2m_Z^2 tu + 6u^2 u_1 + tu^2) - m_1^2 Y(m_1^2 - m_2^2)(8m_Z^2 u_1 \\
& + 10m_Z^2 s + 2su - s^2) - (m_1^2 - m_2^2)s(-2m_Z^4 Y - 6m_Z^6 u - tuY + 3m_Z^4 u^2 + 6m_Z^2 u^3 \\
& - tu^3 - 2u^4) + m_1^2 Y(8m_Z^6 - 2m_Z^2 tu + t^2 u - 6m_Z^2 u^2 - u^3) + \beta_Z \{2(m_2^6 - m_1^6 - m_1^4 m_2^2 \\
& - m_1^2 m_2^4)s^2(m_Z^2 - 3u) + 8sYm_1^6 - 4m_1^2 m_2^2(2m_1^2 - m_2^2)su_1(s - 2u_1) \\
& - 2(m_1^2 - m_2^2)^2 su_1(3u_1^2 - Y) - m_2^2(m_1^2 - m_2^2)sY(6m_Z^2 - t - 9u) \\
& - 2(m_1^2 - m_2^2)u_1^2(-m_Z^4 s_4 - 8m_Z^4 u + 3m_Z^2 su - s^2 u + 4m_Z^2 u^2) \\
& \left. \left. + m_2^2 Y(8m_Z^2 u_1^2 - ss_4 u)\right\} D_{ZZ}^{1211}(s, u) - (u \leftrightarrow t, \beta_Z \rightarrow -\beta_Z) \right] + (1 \leftrightarrow 2) \Big], \quad (\text{A.61})
\end{aligned}$$

$$\begin{aligned}
A_{+-+0}^{(\tilde{x}_1 \tilde{x}_2 2)}(\beta_Z, t, u; m_1^2, m_2^2) = & -\frac{2(t - u + \beta_Z s)}{m_Z^2 s} \left\{ 2sC_0^{111}(s) + \frac{(s + 4m_Z^2)Y}{s_4} D_{ZZ}^{1221}(t, u) \right. \\
& \left. + E_1^{12}(s, u) + E_1^{12}(s, t) - (m_1^2 - m_2^2)s[D_{ZZ}^{1211}(s, u) + D_{ZZ}^{1211}(s, t)] + (1 \leftrightarrow 2) \right\}, \quad (\text{A.62})
\end{aligned}$$

$$\begin{aligned}
A_{++00}^{(\tilde{x}_1 \tilde{x}_2 1)}(\beta_Z, t, u; m_1^2, m_2^2) = & \frac{32m_Z^2}{s_4} \left\{ \frac{2Y}{t_1 u_1} - \frac{1}{su_1^2} [2m_Z^2 Y + (u - t)(u^2 - m_Z^4)] B_Z^{12}(u) \right. \\
& - \frac{1}{st_1^2} [2m_Z^2 Y + (t - u)(t^2 - m_Z^4)] B_Z^{12}(t) - \frac{Y}{s^2} E_2^{12}(t, u) \Big\} + \frac{4}{s_4 m_Z^2} \left[2m_1^2 [8m_Z^4 \right. \\
& - 2s(m_1^2 - m_2^2) + ss_4] C_0^{111}(s) + 2sm_1^2(m_1^2 - m_2^2)^2 \tilde{F}^{12}(s, t, u) + \frac{(m_1^2 + m_2^2)s_4 m_Z^2}{s} E_2^{12}(t, u) \\
& + \frac{1}{s} \left\{ (m_1^4 + m_2^4)s(t + m_Z^2)(u + m_Z^2) + 4(m_1^2 + m_2^2)m_Z^4 Y + 2m_1^2 m_2^2 s[Y + t(t + m_Z^2) \right. \\
& \left. + u(u + m_Z^2)] \right\} D_{ZZ}^{1221}(t, u) + \left\{ \frac{2}{u_1} [8m_Z^6 m_1^2 - u_1^2(m_1^2 - m_2^2)^2] C_Z^{211}(u) \right. \\
& \left. + 2m_1^2 [m_1^2 m_Z^2(4m_Z^2 - 3s) + m_2^2(s_2^2 + sm_Z^2) + 2s_2 m_Z^4] D_{ZZ}^{1211}(s, u) \right.
\end{aligned}$$

$$+(u \leftrightarrow t) \Big\} + (1 \leftrightarrow 2) \Big] , \quad (\text{A.63})$$

$$\begin{aligned} A_{++00}^{(\tilde{\chi}_1 \tilde{\chi}_2^2)}(\beta_Z, t, u; m_1^2, m_2^2) = & -\frac{4}{m_Z^2} \left[2sC_0^{111}(s) + \frac{2m_Z^2}{s} E_2^{12}(t, u) \right. \\ & + (m_1^2 + m_2^2)s_2 \tilde{F}^{12}(s, t, u) - 2m_Z^2(m_1^2 - m_2^2)[D_{ZZ}^{1211}(s, u) + D_{ZZ}^{1211}(s, t)] \\ & \left. + (1 \leftrightarrow 2) \right] , \quad (\text{A.64}) \end{aligned}$$

$$\begin{aligned} A_{+-+}^{(\tilde{\chi}_1 \tilde{\chi}_2^1)}(\beta_Z, t, u; m_1^2, m_2^2) = & -\frac{16[s_2 Y + \beta_Z m_Z^2 s(u-t)]}{s_4 t_1 u_1} \\ & + \frac{8s_2[Y - s(s_4 + \beta_Z(u-t))]}{s_4 Y} [B_Z^{11}(s) + B_Z^{22}(s)] - \frac{4ss_2}{s_4 Y^2} [3m_Z^8 + (t^2 + u^2)(Y - 3m_Z^4) \\ & + t^4 + t^2 u^2 + u^4 - \beta_Z s(t-u)(t^2 + tu + u^2 - 2m_Z^4)][C_0^{111}(s) + C_0^{222}(s)] \\ & + \frac{4s}{s_4 Y^2} \left\{ -s_4[(t^2 - m_Z^4)^2 + (u^2 - m_Z^4)^2 - (tu + m_Z^4)^2 + tus_2^2] \right. \\ & + \beta_Z(t-u)[2Y^2 + (t^2 + u^2)(4Y + t^2 + u^2 - tu) - 2m_Z^4 tu] \Big\} [C_{ZZ}^{121}(s) + C_{ZZ}^{212}(s)] \\ & - \left\{ 16 \left[\left(\frac{m_Z^4(u-t)}{s_4 u_1^2} - \frac{1}{2} \right) (1 - \beta_Z) + \frac{m_Z^2}{s_4} \left(1 - \frac{2m_Z^4}{u_1^2} \right) - \frac{2u\beta_Z}{s_4} - \frac{u^2}{Y s_4} [s_4 \right. \right. \\ & + \beta_Z(u-t)] \Big] B_Z^{12}(u) + \frac{2}{s_4 Y^2} [s_2(Y^2 - 2u^3 s_2) + 4m_Z^4 u(Y + 2u^2) \\ & - \beta_Z s[Y^2 - 2u^2(2m_Z^4 + us_2)]] [E_1^{12}(s, u) + E_1^{21}(s, u)] + (u \leftrightarrow t \quad , \quad \beta_Z \rightarrow -\beta_Z) \Big\} \\ & + \frac{4}{s_4 Y^2} \left[-4Y(m_1^2 - m_2^2)[Y - s(s_4 + \beta_Z(u-t))] B_Z^{11}(s) \right. \\ & - s \left\{ (2Y - ss_4)(m_1^2 - m_2^2)^2 [2(m_1^2 - m_2^2) - 3s_2] - (m_1^2 - m_2^2)[4s_4 Y m_1^2 \right. \\ & + 2m_Z^4(2tu + m_Z^4) + (t^2 + u^2)(4tu - 10m_Z^4) + 4Y^2 + 3(t^4 + u^4)] + 2m_1^2 s_4 s_2 Y \\ & + \beta_Z(u-t) \{ s(m_1^2 - m_2^2)^2 [3s_2 - 2(m_1^2 - m_2^2)] - (m_1^2 - m_2^2)[4Y m_1^2 + s(3(u^2 + t^2) \\ & + 4Y)] + 2s_2 Y m_1^2 \} \Big\} C_0^{111}(s) - s \left\{ s_4(m_1^2 - m_2^2)[4Y + 3(t-u)^2](m_1^2 - m_2^2 - s_2) \right. \\ & + 2m_1^2 s_4^2 Y + \beta_Z(u-t) \{ (m_1^2 - m_2^2)[10Y + 3(t-u)^2](m_1^2 - m_2^2 - s_2) \\ & + 2m_1^2 s_4 Y \} \Big\} C_{ZZ}^{121}(s) + \frac{1}{s} \{ 4m_1^2 m_2^2 m_Z^2 s Y^2 + 2(m_1^4 + m_2^4)s(3m_Z^2 - s)Y^2 \\ & - (m_1^2 + m_2^2)s_2 Y^3 + (m_1^2 - m_2^2)^4 s^2 (2Y - ss_4) + 2(m_1^2 - m_2^2)(m_1^4 - m_2^4)(Y - ss_4)Ys \\ & + \beta_Z s(t-u)(m_1^2 - m_2^2)^2 [s^2(m_1^2 - m_2^2)^2 + 2(m_1^2 + m_2^2)Ys + Y^2] \} D_{ZZ}^{1221}(t, u) \\ & + \left[\frac{2}{su_1} \left\{ su_1^2(m_1^2 - m_2^2)^2 [Y(u_1 - m_Z^2) + 3u(u^2 - 2m_Z^4) + 3tm_Z^4] + (m_1^2 - m_2^2)u_1^2 [2m_Z^8(s - u_1) \right. \right. \\ & \left. \left. - 2m_Z^6 u(t + t_1) + 2m_Z^2 u^2(u - 2m_Z^2)^2 - su^2(14m_Z^4 - s^2 + 2m_Z^2 s + 2us_4)] \right\} \right. \end{aligned}$$

$$\begin{aligned}
& +2Ym_1^2[2m_Z^8(m_Z^2-4u)+m_Z^2s_4(m_Z^4s+s^2u-4m_Z^2u^2)+4m_Z^6u(2s-u)+m_Z^2s^2uu_1 \\
& +u^3(2m_Z^2u+s^2-8m_Z^4)]-\beta_Zs\{u_1^3(m_1^2-m_2^2)^2(Y+3m_Z^2t_1+3uu_1) \\
& +(m_1^2-m_2^2)suu_1^2(4m_Z^4-tu-3u^2)+2m_1^2sY[uu_1(u+m_Z^2)-m_Z^2Y]\}\}C_Z^{211}(u) \\
& -\frac{1}{2}\left\{-2s(m_1^2-m_2^2)^4(2Y-ss_4)+4(m_1^6-m_2^6)s(m_Z^4t-5m_Z^4u-s_2tu+2u^3) \right. \\
& -8Ym_1^6(Y-ss_4)+4m_1^2m_2^2(m_1^2-m_2^2)(2m_Z^8-14m_Z^6s+5m_Z^4s^2-8m_Z^6u+26m_Z^4su \\
& -s^3u+12m_Z^4u^2-10m_Z^2su^2+s^2u^2-8m_Z^2u^3-2su^3+2u^4)+8Ym_1^4m_2^2(Y-ss_4) \\
& +6s(m_1^2-m_2^2)^2(m_Z^8-6m_Z^4u^2+t^2u^2-2u^3s_2)+16Ym_1^4(-m_Z^2Y+m_Z^4t-3m_Z^4u-u^2s_2) \\
& -8Ym_1^2m_2^2(m_Z^4t-7m_Z^4u+us_2^2-u^2s_2)+(m_1^2-m_2^2)s[-m_Z^8s_2-10um_Z^4Y-2m_Z^4t^2u \\
& +t^3u^2-u^3(4Y-8ss_4+t^2)]+2Ym_1^2[-m_Z^4(8Y+s_2^2+16u^2)+6t^2u^2+9tu^3+4u^4+t^3u] \\
& -\beta_Zs\{2s(m_1^2-m_2^2)^4(t-u)+4s(m_1^4-m_2^4)(m_1^2+m_2^2)(m_Z^4+tu-2u^2)+8Y(t-u)m_1^6 \\
& -32m_1^4m_2^2u_1(uu_1+m_Z^2t_1)-8m_1^2m_2^4(2m_Z^6-3m_Z^4s+6m_Z^2uu_1+s^2u+3su^2-2u^3) \\
& -(m_1^2-m_2^2)[12su(m_1^2-m_2^2)(u^2-m_Z^4)+16Ym_1^2(u^2-m_Z^4)+sY^2+4su^2(Y \\
& +2(u^2-m_Z^4))]-2m_1^2Y[tY+u(3Y+4(u^2-m_Z^4))]\}\}D_Z^{1211}(s,u) \\
& + (u \leftrightarrow t \ , \ \beta_Z \rightarrow -\beta_Z) \Big] + (1 \leftrightarrow 2) \Big] , \tag{A.65}
\end{aligned}$$

$$A_{+-+}^{(\tilde{\chi}_1\tilde{\chi}_22)}(\beta_Z, t, u; m_1^2, m_2^2) = \frac{8}{s_4} \left\{ 2Y - s[s_4 + \beta_Z(t-u)] \right\} D_Z^{1221}(t, u) . \tag{A.66}$$

References

- [1] ALEPH, DELPHI, L3 and OPAL Collaborations, The LEP working group for Higgs boson searches, CERN-EP-2000-055; P. Igo-Kemenes, Search for New Particles and New Phenomena Results from e^+e^- Colliders, talk presented at XXXth International Conference on High Energy Physics, August 2000, Osaka, Japan, <http://ichep2000.hep.sci.osaka-u.ac.jp>
- [2] D.L. Borden, D.A. Bauer and D.O. Caldwell, Phys. Rev. **D48**, 1993 (4018); M. Bailargeon, G. Belanger and F. Boudjema, hep-ph/9405359; J.F. Gunion, in Perspectives on Higgs Particles, hep-ph/9705282;
- [3] I.F. Ginzburg, G.L. Kotkin, V.G. Serbo and V.I. Telnov, Nucl. Instr. and Meth. **205**, 47 (1983); I.F. Ginzburg, G.L. Kotkin, V.G. Serbo, S.L. Panfil and V.I. Telnov, Nucl. Instr. and Meth. **219**,5 (1984); J.H. Kühn, E.Mirkes and J. Steegborn, Z. f. Phys. **C57**, 615 (1993).
- [4] Opportunities and Requirements for Experimentation at a Very High Energy e^+e^- Collider, SLAC-329(1928); Proc. Workshops on Japan Linear Collider, KEK Reports, 90-2, 91-10 and 92-16; P.M. Zerwas, DESY 93-112, Aug. 1993; Proc. of the Workshop on e^+e^- Collisions at 500 GeV: The Physics Potential, DESY 92-123A,B,(1992), C(1993), D(1994), E(1997) ed. P. Zerwas; E. Accomando *et.al.* Phys. Rep. **C299**, 299 (1998).
- [5] M. Melles, hep-ph/0008125.
- [6] E.W.N. Glover and J.J. van der Bij, Nucl. Phys. **B321**, 561 (1989).
- [7] G. Jikia Nucl. Phys. **B405**, 24 (1993).
- [8] G.J. Gounaris, J. Layssac, P.I. Porfyriadis and F.M. Renard, hep-ph/9909243, Eur. Phys. J. **C13**, 79 (2000).
- [9] G.J. Gounaris, P.I. Porfyriadis, F.M. Renard, hep-ph/9812378, Phys. Lett. **B452**, 76 (1999), Phys. Lett. **B464**, 350 (1999) (E); G.J. Gounaris, P.I. Porfyriadis, F.M. Renard, hep-ph/9902230, Eur. Phys. J. **C9**, 673 (1999).
- [10] G.J. Gounaris, J. Layssac, P.I. Porfyriadis and F.M. Renard, hep-ph/9904450, Eur. Phys. J. **C10**, 499 (1999).
- [11] H. Nilles, Phys. Rep. **110**, 1 (1984); H.E. Haber, and G.L. Kane Phys. Rep. **117**, 75 (1985); J. Rosiek, Phys. Rev. **D41**, 3464 (1990), hep-ph/9511250(E); M. Kuroda, hep-ph/9902340.
- [12] J.F. Gunion, H.E. Haber, G. Kane and S. Dawson, "The Higgs Hunter's Guide", Addison-Wesley, Redwood City (1990).

- [13] A. Djouadi, V. Driesen, W. Hollik and J.I. Illana, Eur. Phys. J. **C1**, 163 (1998).
- [14] M.M. Mühlleitner, M. Krämer, M. Spira and P.M. Zerwas, talk at the International Workshop on High Energy Photon Colliders, June 14-17, 2000, DESY Hamburg, Germany, to appear in Nucl.Instr. & Meth. A.; M.M. Mühlleitner, Dissertation at the University of Hamburg, hep-ph/0008127; H. E. Haber *et.al.* hep-ph/0007006.
- [15] D.A. Dicus and C. Kao, Phys. Rev. **D49**, 1265 (1994).
- [16] G. Passarino and M. Veltman, Nucl. Phys. **B160**, 151 (1979).
- [17] K. Hagiwara, S. Matsumoto, D. Haidt and C.S. Kim, Z. f. Phys. **C64**, 559 (1995).
- [18] H. Haber, R. Hempfling, prl6618151991; Y. Okada, M. Yamaguchi, T. Yanagida, Prog. Theor. Phys. **85**, 1 (1991); J. Ellis, G. Ridolfi, F. Zwirner, Phys. Lett. **B257**, 83 (1991); *ibid* Phys. Lett. **B262**, 477 (1991); R. Barbieri, M. Frigeni, Phys. Lett. **B258**, 395 (1991); S. Heinemeyer, W. Hollik and G. Weiglein, Phys. Lett. **B455**, 179 (1999), hep-ph/9903404.
- [19] V. Telnov, hep-ex/0003024, hep-ex/0001029, hep-ex/9802003, hep-ex/9805002, hep-ex/9908005; I.F. Ginzburg, hep-ph/9907549; R. Brinkman hep-ex/9707017.
- [20] V. Telnov, talk at the International Workshop on High Energy Photon Colliders, <http://www.desy.de/~gg2000>, June 14-17, 2000, DESY Hamburg, Germany, to appear in Nucl.Instr. & Meth. A.
- [21] C. Quigg, Talk dedicated to the memory of Sam Treiman, hep-ph/0001145.
- [22] A. Djouadi, S. Rosier-Lees (editors) *et.al.* "The Minimal Supersymmetric Standard Model: Group Summary Report", hep-ph/9901246; V. Barger *et.al.* "Report of SUGRA Working Group for Run II of the Tevatron", hep-ph/0003154.
- [23] A. Djouadi, J. Kalinowski and M. Spira, HDECAY, hep-ph/9704448, Comput. Phys. Commun. **108**, 56 (1998).
- [24] G.-C. Cho, K. Hagiwara, Nucl. Phys. **B574**, 623 (2000).
- [25] M. Jacob and G.C. Wick, Ann. Phys. (N.Y.) **7**, 404 (1959).
- [26] G.J. Gounaris and P.I. Porfyriadis, hep-ph/0007110, to appear in Eur. Phys. J. C.
- [27] G.J. Gounaris, J. Layssac and F.M. Renard, hep-ph/0003143, Phys. Rev. **D62**, 073013 (2000).

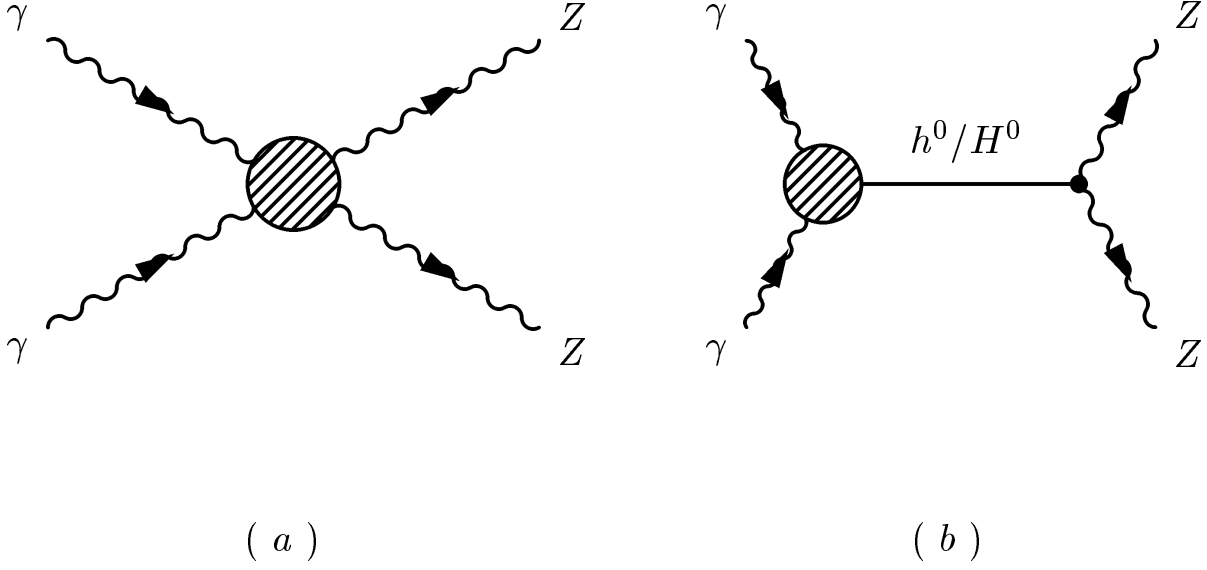


Figure 1: Feynman Diagrams for the $\gamma\gamma \rightarrow ZZ$ process.

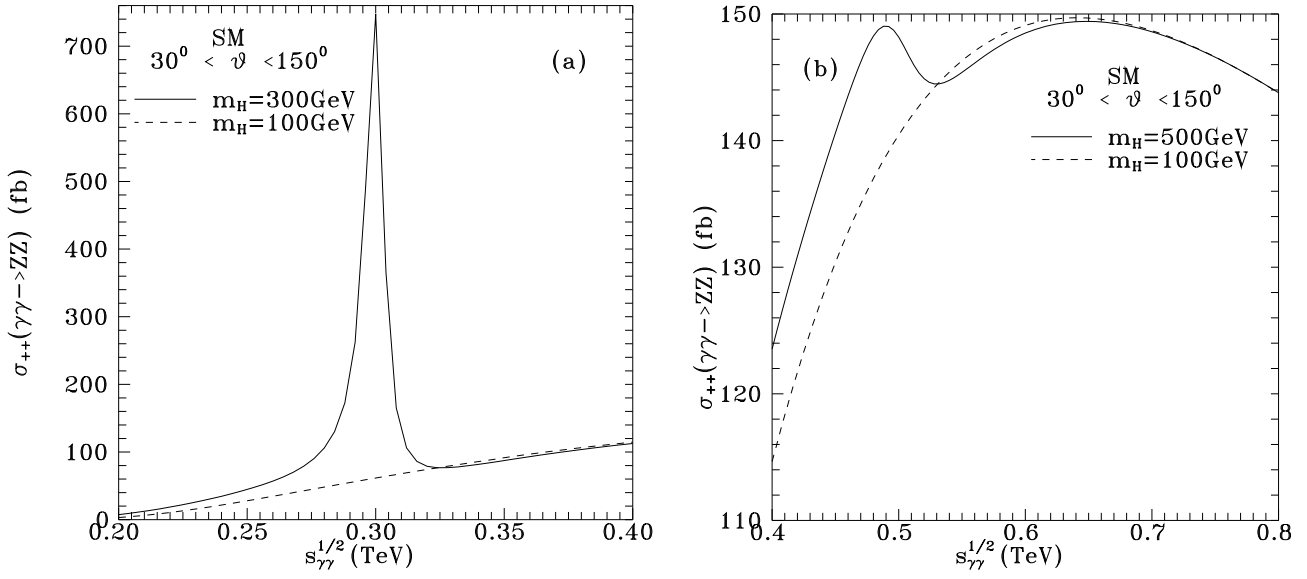


Figure 2: SM contribution to the $\sigma_{++}(\gamma\gamma \rightarrow ZZ)$ cross section. Solid lines are for $m_H = 300$ GeV (a) and $m_H = 500$ GeV (b), while dash lines give the results for $m_H = 100$ GeV in both (a) and (b).

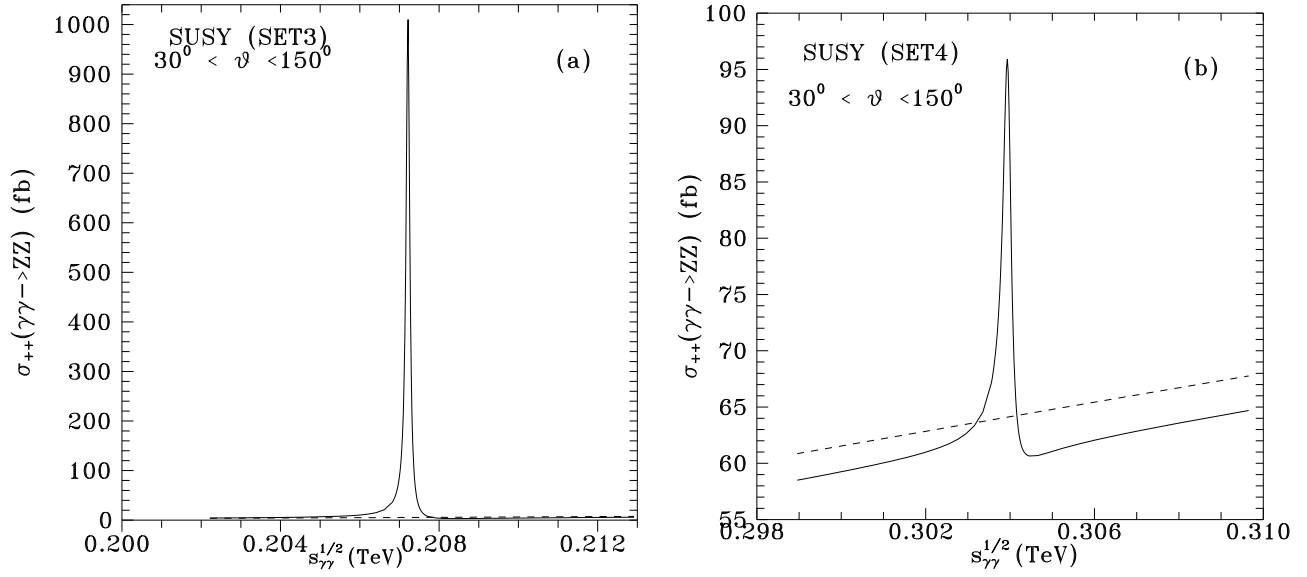


Figure 3: Solid lines describe SUSY predictions for the parameters of Set3 (a) and Set4 (b) in Table 1. Dash lines present the SM results for $m_H = 100$ GeV.